LEGIBILITY NOTICE

A major purpose of the Technical Information Center is to provide the broadest dissemination possible of information contained in DOE's Research and Development Reports to business, industry, the academic community, and federal, state and local governments.

Although a small portion of this report is not reproducible, it is being made available to expedite the availability of information on the research discussed herein.

ORNL/tr--88/25

DE89 001721

DEVELOPMENT AND STUDY ON AN ELECTROREDUCTION MIXER-SETTLER FOR SEPARATION OF PLUTONIUM DURING REPROCESSING OF NUCLEAR FUELS

By Helmut Schmieder

Translated from the French* Microfilm of thesis presented to the Grenoble National Polytechnical Institute September, 1984, for the degree of Doctor, Chemical Engineering

Prepared for the
OAK RIDGE NATIONAL LABORATORY
Oak Ridge, Tennessee 37831
operated by
MARTIN MARIETTA ENERGY SYSTEMS, INC.
for the
U.S. DEPARTMENT OF ENERGY
under Contract No. DE-AC05-84OR21400

*Translated by LANGUAGE SERVICES, Nashville, TN for Oak Ridge National Laboratory

Attention Microfiche User,

The original document from which this microfiche was made was found to contain some imperfection or imperfections that reduce full comprehension of some of the text despite the good technical quality of the microfiche itself. The imperfections may be:

- missing or illegible pages/figures
- wrong pagination
- poor overall printing quality, etc.

We normally refuse to microfiche such a document and request a replacement document (or pages) from the National INIS Centre concerned. However, our experience shows that many months pass before such documents are replaced. Sometimes the Centre is not able to supply a better copy or, in some cases, the pages that were supposed to be missing correspond to a wrong pagination only. We feel that it is better to proceed with distributing the microfiche made of these documents than to withhold them till the imperfections are removed. If the removals are subsequently made then replacement microfiche can be issued. In line with this approach then, our specific practice for microfiching documents with imperfections is as follows:

1. A microfiche of an imperfect document will be marked with a special symbol (black circle) on the left of the title. This symbol will appear on all masters and copies of the document (1st fiche and trailer fiches) even if the imperfection is on one fiche of the report only.

2. If imperfection is not too general the reason will be specified on a sheet such as this, in the space below.

3. The microfiche will be considered as temporary, but sold at the normal price. Replacements, if they can be issued, will be available for purchase at the regular price.

4. A new document will be requested from the supplying Centre.

5. If the Centre can supply the necessary pages/document a new master fiche will be made to permit production of any replacement microfiche that may be requested.

The original document from which this microfiche has been prepared has these imperfections:

☐ missing pages/figures numbered: _____

☐ wrong pagination

☒ poor overall printing quality

☐ combinations of the above

☐ other

INIS Clearinghouse
IAEA
P. O. Box 100
A-1400, Vienna, Austria

[Translator's Note: In addition to the poor printing quality of this thesis which make the tables impossible to read, it should be noted that, according to the author's foreword, the thesis itself is a translation from German.

The errata inserted at the beginning of the thesis have been accounted for in the translation itself.

Two unnumbered pages at the beginning list the faculty of the Grenoble National Polytechnical Institute.

Two pages at the end constitute official permission for the thesis to be presented and defended.]

DEVELOPMENT AND STUDY OF AN ELECTROREDUCTION MIXER-DECANTER FOR SEPARATION OF PLUTONIUM DURING THE REPROCESSING OF NUCLEAR FUELS

Table of Contents

CHAPTER IV: DISCUSSION OF RESULTS

INTRODUCTION

1. Foreword

According to the forecasts of the last two energy conferences, we can expect insufficient energy production in the next century unless nuclear energy is developed on a large scale, specifically the breeder reactor type which conserves uranium. It appears that current developments, particularly on breeders, is more than hesitant. Only France is an exception, as is shown by the satisfactory operation for years of the PHENIX reactor as well as the construction of the SUPER PHENIX. It is, therefore, an honor for me to present this work to the National Polytechnical Institute in Grenoble. I thank Professor Besson very sincerely.

The research and experiments described in this work were done in close collaboration with a group of technicians and engineers from the Institut für Heisse Chemie of the Karlsruhe Nuclear Research Center. Without them and the support of the initiator of the development project, Professor F. Baumgartner, the current results would not have been achieved. I would also like to thank Dr. Petrich of the Institut für Heisse Chemie for the simulation calculations and Mr. Vasamiliette for the translation.

Finally, I would like to express my thanks to the persons who were kind enough to take an interest in this work and participate in the examination jury. Mr. L. Bonnetain, Professor at the National Polytechnical Institute in Grenoble, Mr. J. Spitz, Chairman of the Department of Metallurgy of the Grenoble Nuclear Research Center and Mr. F.J. Hermann, head of the department at the W.A.K. Company as well as Mrs. S. Jordan who was willing to type the text competently and quickly.

2. Method of Reprocessing Nuclear Fuel

The history of reprocessing nuclear fuels began in the United States in the mid 1940s with the production of plutonium by precipitation according to the well-known bismuth phosphate process. Following that, other extraction methods, particularly by aqueous means, were developed that finally resulted in the Purex process that is used today worldwide. The largest facility in service reprocessing light water reactor fuel is at La Hague in France.

This method is based on an extraction by tributyl phosphate (T.B.P.) from nitric solutions. By diluting the T.B.P. with approximately 30% volume of kerosene (essential component n-dodecane), a sufficiently great density difference is reached between the organic and aqueous media to obtain good separation of the two phases in the extractors. For this separation, mixer-settlers, pulsed columns or centrifugal extractors can be used. Our research treats the use of mixer-settlers.

Spent fuel contains fission products and transuranian elements. After discharge from a light water reactor, the radioactivity of the fission products reaches 10^7 curies/t of metal for a normal burnup rate of 34 000 MW.day/ton. The hard gamma radiation of the radioactive elements imposes the use of lead and concrete shielding for handling these fuels. On the other hand, the heat of decay of the recently discharged (fuel) rods reaches over 60 kW/t and requires that they be stored in (cooling) ponds. The radioactivity and heat of decay decrease greatly with immersion time, on the average of one order of magnitude during the two years after discharge.

In a light water reactor, the plutonium content of the fuel is about 0.9 g %. When this plutonium is to be reused in a reactor of the same type, the oxide PuO_2 is added until the Pu content reaches 3-4 g. For the breeder core elements, it can go as high as 20 g %. The standards imposed for Pu and U prior to fuel refabrication or enrichment require decontamination factors (DF)[1] during reprocessing of up to 10^7 for short fuel cooling times (< 1a). Thus, the Pu contamination of uranium cannot exceed 15 000 α decays per g. min, which corresponds to 0.1 μg Pu - 239 gram.

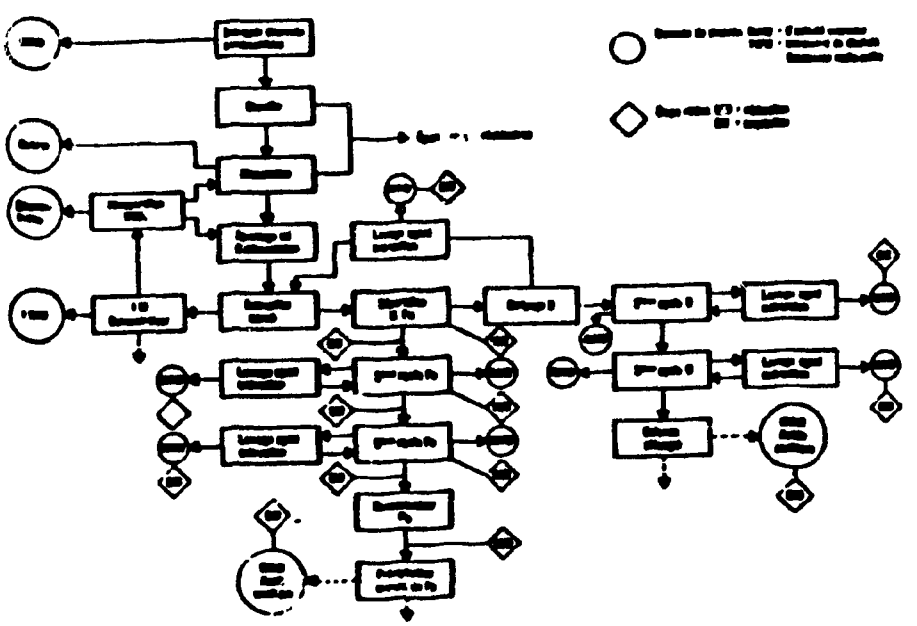

Figure 1 - [all printing illegible]

[1] $DF = \frac{\text{Impurity concentration before purification}}{\text{Impurity concentration after purification}}$

Figure 1 gives a flow chart of the complete process. From the cooling tank of the reactor, the fuel elements are transferred to a basin in the reprocessing facility. Once the rods have been sawed up, the fragments go into a disolving process in 8 M nitric acid where the oxidized fuel is freed from the cladding. The solution, which has a concentration of approximately 3 M of HNO_3, is then introduced into a first extractor where the U and Pu go into the organic phase while over 99% of the fission products are eliminated with the aqueous phase. The organic phase then passes into a second extractor where a new fraction of the fission products is separated from them (washing). Then the U and Pu are separated in a third extractor where the extractable Pu(IV) is reduced to practically non-extractable Pu(III) which is taken up by the aqueous phase, while the U(VI) that has remained in organic phase is reextracted in a fourth extractor by a diluted solution of nitric acid.

After this first cycle, the U and Pu are separated from the fission products with a decontamination factor DF of 10^4. They are also separated from each other with a DF of 10^3 to 10^4. Before reaching the above standards, the U and Pu must still undergo two purification cycles. The uranium is extracted and the washing of the fission products handled in a combined extractor. In the next extractor, the U is reextracted with a dilute solution of nitric acid.

The process is the same in the second and third plutonium cycles. For some time, a reducing reextraction is performed in each cycle in order to increase the Pu concentration. In the traditional method with diluted nitric acid, Pu concentrations of only about 15 $g.l^{-1}$ are reached. The Pu is then precipitated by the oxalic acid and the plutonium oxalate is finally transformed by

calcination into plutonium dioxide prior to being sent to refabrication. The uranium solution is often filtered on a silica gel bed, in order to eliminate the remaining fission products, particularly zirconium.

The two phases involved in the process are recycled. The organic extraction medium is subjected to an alkaline washing in order to eliminate from it the hydrogen phosphates formed by radiolysis and hydrolysis of TBP The nitric acid is recycled by evaporation as quantitatively as possible in order to reduce both the Pu and U losses and the volume of low and medium activity wastes.

It should also be mentioned that, between the two cycles, the plutonium previously reduced to the III degree must be reoxidized to reextractable Pu(IV). In figure 1 the oxidation state changes are symbolized by diamonds while the potential sources of wastes are shown by circles.

3. Problem: Separation of Plutonium by Electroreduction and Counter-Current Extraction

The traditional reducing agent of Pu(IV) in the PUREX process is ferrous sulfamate. Although this stage of the process has proven itself technically for low Pu contents (burnup rate of several hundred MW d/t), it is not indicated for the higher Pu concentrations present in light water reactor and breeder fuels. In fact, in order to reach a complete separation of the plutonium, this stage requires a great excess of the reducing agent (20-40 times the stoichiometric quantity), as predicted by thermodynamic calculations from the standard potentials (3). In addition, the ferrous salt cannot be

recycled and, therefore, must be treated as a radioactive waste, thereby seriously compromising the economics of the process.

Therefore, used today as reducing agent of the U(IV) which is produced by electrolytic means outside the extractor. [Trans. note: incomplete sentence] The U(IV) solution is protected from oxidation by the reduction products of the nitric acid (NO^-_2 and N_2O_4) by adding hydrazine. In the case of Fe(11), this role is played by the sulfamate ion itself which reduces the nitrites to nitrogen, with formation of sulfate.

In fact, the practice of reduction by U(IV) revealed some weakness as to its effectiveness. In the event the uranium is not regularly distributed along the extractor by introducing it in at least two points, insufficient Pu separation is observed, as well as, occasionally, the spontaneous oxidation of the Pu(III) and of the reducing agent (4,5). The two effects are the result of the local depletion of U(IV) and/or hydrazine. Although the equilibrium constant, calculated from the standard potentials (see also Appendix III), is very high, a uranium excess of approximately 5 times the stoichiometric quantity is required in practice in order to achieve a total separation of the plutonium. This has a bad influence on reprocessing of breeder fuel because, for a Pu rate of 20% mass, over half of the total uranium must be recycled constantly in the form of U(IV).

Given the problems of the methods of reduction by ferrous sulfamate as by U(IV), it is not surprising that for over 10 years there has been an attempt to replace them by electroreduction in the extraction device (6,7,8). In fact, in this technique no radioactive waste is formed and no local depletion of the reducing agent is likely to take place, since, considering the structure of the

cells (see below), the same reducing conditions exist at all points of the apparatus.

With the setup of a mixer-settler equipped for electroreduction in the second Pu cycle at the WAK Company reprocessing facility (annual capacity of 35 T of fuel), an intermediary stage of development was reached in 1980.

Since then, this mixer-settler has been proven during several campaigns.[2]

In this research, we propose to describe the construction and the performance levels of our electroreduction mixer-settler. We also developed a mathematical model that attempts to represent the complex phenomena of extraction and oxidation-reduction, phenomena whose bases will be discussed in the first chapter.

Developmental research on electroreduction devices has also been done in the United States (9) and France (10).

[2] In fact it appears that, for industrial practice, pulsed columns will be prefered in the future to the mixer-settler system we studied. However, our work has the virtue of being applicable to an existing industrial facility and of supplying a basis that allows the development of a simulation method applicable to a plused column as well.

CHAPTER I

CHEMICAL AND ELECTROCHEMICAL BASES OF THE PROCESS

I - 1. Balance of distribution in the H_2O/TBP system

In the initial attack solution, the uranium is in the form of uranyl nitrate with a valence of 6 and of plutonium nitrate with a valence of 4. With the TBP, these two compounds form stable complexes with the chemical formula: $UO_2(NO_3)_2$, 2TBP and $Pu(NO_3)_4$, 2TBP. Since they are hydrophobic, these complexes are particularly soluble in organic phase. As for the fission products, if they do it at all, with TBP they form only complexes that are much less stable than U(VI) and PU(IV) and then pass into aqueous phase. This partition difference makes it possible to separate U and Pu from the fission products. The corresponding partition coefficient[3] depends on various parameters such as the acid concentration, the TBP concentration, the temperature and the concentration of metal ions. Under these circumstances, the ions that form complexes with the TBP are in competition with each other.

Figure 2 illustrates the variation of the partition coefficients with the acidity for several metal ions in low concentrations. These coefficients are determined for a concentration of 30% by volume of TBP. As a dilutant, kerosene (mixture of aliphatic hydrocarbons with C-10, C-13), turned out to be the cheapest and more resistant than branched hydrocarbons and other cyclic paraffins. Its relatively low vapor pressure, as well as its sufficiently high

---

[3] $D_a = \frac{\text{Concentration in the organic phase}}{\text{Concentration in the acqueous phase}}$

flame point, contribute to reducing the dangers of fire and explosion. For this concentration of 30% by volume of TBP dissolved in kerosene and a nitric acid concentration of 3 $M.l^{-1}$, the partition coefficient at 25°C is about 20 for U(VI), 10 for Pu(IV) and only 0.2 for the zirconium that is one of the fission products. Among the latter, only ruthenium, niobium and cerium have a partition coefficient close to that of zirconium, while the others are still less soluble in the organic phase.

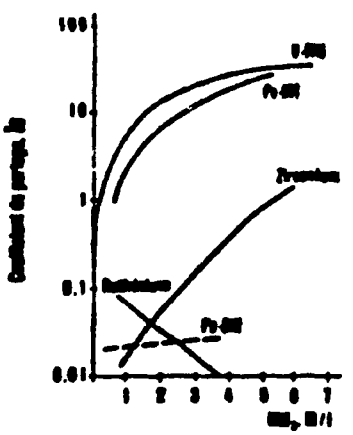

Fig. 2 [illegible]

Fig. 2 Partition Coefficient as a function of the nitric acid content [illegible]

In addition, as shown by Figure 2, the partition coefficient of ruthenium decreases as the acidity increases whereas that of zirconium increases. Their intersection is at a HNO_3 concentration of approximately 2 $M.l^{-1}$. Therefore, it is this concentration that will be optimal as for the separation of Zr-Ru on the one hand, U and Pu on the other hand and, more generally, for the elimination of fission products.

However, other phenomena depending on the acid concentration must also be accounted for. Specifically, by radiolysis of the TBP, decomposition products (dibutylic phosphate) form that produce precipitates with zirconium, The latter accumulate in the boundary layers of the two phases in the extractors and can provoke their obstruction. This tendency to precipitation decreases with an increase of the acidity, which leads to adopting for extraction an acid concentration of the initial attack solution of 3 $M.l^{-1}$ rather than of 2 $M.l^{-1}$ which would be ideal for the elimination of the fission products.

Figure 2 also shows the partition coefficient of Pu(III). It is two orders of magnitude smaller than that of Pu(IV). It is then possible to separate the uranium from the plutonium by reduction of the latter to the III degree. The partition coefficient of U(IV), which is the reducing agent in most current facilities, is approximately ten times less than that of U(VI). With 30% volume of TBP in the organic phase, a maximum saturation degree of the extraction agent of about 125 $g.l^{-1}$ of U and Pu is achieved. In the industrial extraction facilities, however, this concentration is only about 70% of the theoretical value (or 87.5 $g.l^{-1}$) for hydrodynamic reasons. Finally, it will be noted that a high saturation of U and Pu in the extractant is desirable not only because of the specific flow rate reached but also because it promotes obtaining high decontamination rates for fission products. Thus, for a saturation of 80% uranium, the partition coefficients of the zirconium and ruthenium are ten times smaller than those given in Figure 2.

Temperature also influences the partition equilibrium. The partition coefficients decrease by a half from 30°C to 60°C for a low saturation of the organic phase, but this variation is less pronounced for higher concentrations. There-

fore, extraction is performed at a sufficiently low temperature, around ambient temperature of the extraction cell, or about 30°C. On the other hand, elimination of the fission products is facilitated at higher temperature. Specifically, the distribution equilibrium is displaced in favor of the aqueous phase. That is why the fission products are generally washed at a higher temperature.

Reextraction of the uranium from the organic medium is performed using a highly dilute solution of nitric acid (0.1 $M.l^{-1}$). As Figure 2 shows, the partition coefficient of uranium decreases quickly for acid concentrations below 1 $M.l^{-1}$. In addition, reextraction is performed at a higher temperature (about 60°C) which reduces this partition coefficient still further.

As for the extraction of the Pu and the U, Figure 2 shows that, for an extraction stage (corresponding to the mixture of two equal volumes of the aqueous and organic phases), approximately 90% of the Pu for which the partition coefficient is 10 passes into organic phase, for a concentration of 3 $M.l^{-1}$ of HNO_3. As for the uranium, approximately 95% are extracted under these conditions. However, these values are established for concentrations below 0.1 $M.l^{-1}$ of metal ions. In practice, we have much more concentrated solutions, of about 1 $M.l^{-1}$ for example, in the initial attack solution. Now, for high concentrations in the two phases, that is, for an increasing saturation of the organic phase, the partition coefficients drop greatly, so that per stage only 50% of the U and the Pu are transferred to the organic phase. In practice, the quantitative extraction is technically performed in multi-stage extraction extrac-

tors. It is preferable to work against the current, as in the adsorption (gas-liquid) or rectification (vapor-liquid) processes.

Appendix 1 develops the principles of counter-current extraction of a single extractable component in multi-stages. The difficulty of the mathematical treatment of the partition of several species in the PUREX process resides in the fact that the partition coefficients depend greatly not only on the concentration itself of the complexes extracted and on all other extractable species (U(VI), U(IV), Pu(IV), Pu(VI), Np, fission products, HNO_3), but also on the concentration of the non-extractable components such as hydrazinium nitrate and ammonium nitrate. An entire set of experimental determinations of partition coefficients previously published (11, 12), allowed us to develop a mathematical model (11, 13, 14, 15, 16) based on the equilibria of formation of complexes of each component, correctly simulating the operation of the mixer-settler (17).

Using measurements of the transport coefficient by the single drop method (18), we can also describe approximately the operation of mixers-decanters in which the extraction equilibrium is not reached in the mixer (plateau efficiency < 100%) which is the general case in technical facilities (19). Our model will be described in more detail in Chapter IV, Discussion of Results.

I - 2. Potentials of the various redox pairs of Pu, U, HNO_3, hydrazine and their interreactions

I - 2.1. Plutonium

The chemistry of Pu in aqueous solution is characterized by the simultaneous presence of the oxidation states III, IV, V, VI. The oxidation-reduction potentials of the corresponding redox pairs in acid solution are fairly close. The standard potentials are the following in mV compared to the normal hydrogen electrode, for an acid concentration d of 1 M at 25°C (3):

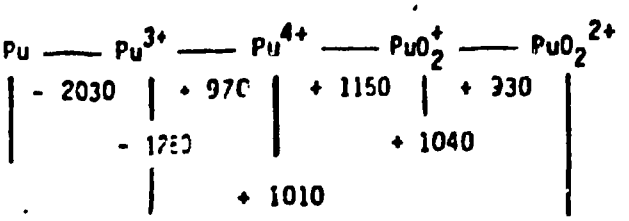

In a nitric medium, the potential of the pair Pu^{4+}/Pu^{3+} deviates considerably from its standard value. In addition, PuO^{+}_2 is unstable in 1M nitric acid (21).

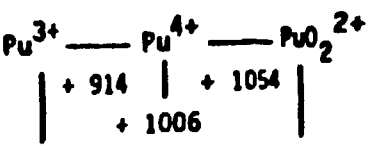

The reason for this is the complexing of Pu^{4+} by the nitrate anion (29). In nitrate solution, Pu^{4+} is stabilized by the permanent presence of nitrous acid, produced by photolysis or by radiolysis, oxidizing Pu^{3+} to Pu^{4+} (22) (see below). During separation by reduction in the PUREX process, a reagent (hydrazine) that reacts quickly with nitrous acid must be used, in order to ensure the stability of Pu(III).

COHEN (23) has examined obtaining the various oxidation numbers of Pu electrochemically in a cell with compartments separated by diaphragms. Starting with a determined oxidation number, he recorded stationary curves of current density as a function of voltage (voltamperograms) in a 1M solution of perchloric acid and noted the following facts:

— The half-wave potentials of the pairs Pu^{3+}/Pu^{4+} and PuO^{+}_{2}/PuO^{2+}_{2} differ very little from the values of the redox potentials. The electron transfers are, therefore, quick.

— The two transitions exhibit an S shape in the voltamperograms with a limit current density characteristic of a process controlled by material transport.

— Oxidation of Pu^{4+} to PuO^{+}_{2} and the reduction of PuO^{+}_{2} to Pu^{4+} require considerable overvoltages that are explained by the change of molecular structure.

I - 2.2. Uranium

The standard calculated potential of the pair U^{4+}/UO^{2+}_{2}:

$$UO_2^{2+} + 4H^+ + 2e^- \rightleftharpoons U^{4+} + 2H_2O \qquad (1)$$

according to thermodynamic data is 0.33 V (ESH) (3). KOLTHOFF and HARRIS (24,25) have proposed the mechanism following the electrochemical reduction of U(VI) to U(IV), involving a reduction stage of U(VI) to U(V) followed by a dismutation stage:

$$UO_2^{2+} + e^- \rightleftharpoons UO_2^+ \qquad [2]$$

$$2UO_2^+ + 2H^+ \rightleftharpoons UO_2^{2+} + UO^{2+} + H_2O \quad \text{(dismutation)} \qquad [3]$$

After polarographic studies performed in perchloric acid, it is clear that the dismutation stage controls the speed of the reaction.

In an earlier study (26) we have shown that, on platinum or titanium cathodes, the reduction of uranium (VI) in nitric acid solution takes place irreversibly with high overvoltages (500 - 600 mV for Ti). In typical cells, the kinetics of formation of U(IV), at a constant current and at high cathode current densities, practically obeys a law of the first order compared to U(VI). The inverse reaction of anode oxidation of U(IV) has been observed only with simultaneous release of oxygen.

U(IV) is an excellent reduction agent of Pu(IV). The reaction is written as follows:

$$2\,Pu^{4+} + U^{4+} + 2H_2O \rightarrow 2Pu^{3+} + UO_2^{2+} + 4H^+ \qquad [4]$$

NEWTON was the first to examine the kinetics of this reaction in perchloric acid (27). He formulates the following law of rates:

$$\frac{d\,|Pu^{4+}|}{dt} = -k\;|Pu^{4+}|\;|U^{4+}|\;|H^+|^{-2} \qquad [5]$$

On the other hand, accounting for the hydrolysis of Pu^{4+} and U^{4+} ions to $Pu(OH)^{3+}$ and $U(OH)^{3+}$:

$$|U^{4+}| = \frac{|U\ IV||H^+|}{(|H^+| + K_{HU})} \quad \text{et} \quad |Pu^{4+}| = \frac{|Pu\ IV||H^+|}{(|H^+| + K_{HP})} \qquad [6]$$

where K_{HU} and K_{HP} represent respectively the hydrolysis constants of U^{4+} and Pu^{4+}, whence the following:

$$\frac{d|Pu\ IV|}{dt} = \frac{k|Pu\ IV||U\ IV|}{(|H^+| + K_{HP})(|H^+| + K_{HU})} \qquad [7]$$

The hydrolysis constants are taken from the literature (28, 29). The activation energy of this reaction is estimated at 104.3 $kJ.Mol^{-1}$. The reaction rate is very fast and its constant has a value of 2175 $Mol.l^{-1}.min^{-1}$ at 20° C.

BIDDLE et al. (30) also examined the kinetics in nitric acid by polarography. It appears that the law of rate for measurable species (equation [7]) also describes, with good approximation, the progress of the reaction without having to consider the complexing of Pu(IV) and U(IV) by the nitrate ion (Pu complexation constant):

$$K_{DP} = \frac{|Pu^{4+}||NO_3^-|}{|Pu(NO_3)^{3+}|} \sim 0.35\ M \text{ (at } 30°C)$$

By recalculating at 20°C the reaction rate constant measured at 0°C using the activation energy according to NEWTON, a value of 3711 $MOL.l^{-1}.min^{-1}$ is obtained, considerably above that of NEWTON in perchloric acid solution.

Also in the organic phase, PU(IV) is reduced by the U(IV) extracted, although considerably slower than in aqueous phase. Polarographic studies by BIDDLE et al. (31) indicate that the rate of this reduction depends very greatly on the water content of the organic phase. The following equation is valid as a first approximation for TBP at 30% by volume:

$$\frac{d|Pu\ IV|_{org}}{dt} = -k \frac{|Pu\ IV|_{org}\ |U\ IV|_{org}}{|H^+|^2_{org}} \qquad [8]$$

Since the measurements were only taken at 0°C, the activation energy is unknown. When the H^+ ion concentration becomes very low, this formula is no longer valid and must be corrected empirically to:

$$\frac{d|Pu(IV)|_{org}}{dt} = -k \frac{|Pu(IV)|_{org}\ |U(IV)|_{org}}{(|H^+|_{org} + 0.05)^2} \qquad [8b]$$

I - 2.3. Nitric Acid

Considering the standard potentials of the redox pairs of nitrogen, we should expect to observe a considerable number of reductions of the nitric acid and of its reduction products at the cathode, under the conditions where U/Pu separation takes place in the extractor. The following list gives some of these potentials (3).

$$NO_3^- + 3H^+ + 2e^- \rightleftharpoons HNO_2 + H_2O \qquad +0.94\ V \qquad [9]$$

$$NO_3^- + 4H^+ + 3e^- \rightleftharpoons NO + 2H_2O \qquad +0.96\ V \qquad [10]$$

$$2NO_3^- + 4H^+ + 2e^- \rightleftharpoons N_2O_4 + 2H_2O \qquad + 0,80\ V \qquad [11]$$

$$HNO_2 + H^+ + e^- \rightleftharpoons NO + H_2O \qquad + 1,00\ V \qquad [12]$$

$$NO_3^- + 10H^+ + 8e^- \rightleftharpoons NH_4^+ + 3H_2O \qquad + 0,88\ V \qquad [13]$$

However, in the presence of hydrazine, the reduction of the nitric acid is stopped, as our previous measurements of efficiency in current (26). The mechanism of electroreduction of the nitric acid proposed by VETTER and PLIETH (32) gives an explanation of this fact. This mechanism involves the following reactions:

$$\left.\begin{array}{l} HNO_2 + H^+ \rightarrow NO^+ + H_2O \\ NO^+ + NO_3^- \rightarrow 2NO_2 \\ (H^+ + NO_2 \rightarrow HNO_2^+) \times 2 \end{array}\right\} \text{(étapes chimiques)} \qquad [14]$$

$$(HNO_2^+ + e^- \rightarrow HNO_2) \times 2 \quad \text{(étape de transfert)}$$

This formulation shows that the electrochemical reduction of nitric acid assumes the presence of nitrous acid. But, in the presence of hydrozine, nitrous acid also reacts very quickly according to the following reactions and thus prevents the electrochemical reduction of HNO_3:

$$N_2H_5^+ + HNO_2 \rightarrow HN_3 + 2H_2O + H^+ \qquad [15]$$

or, with an excess of HNO_2:

$$\frac{3}{2} N_2H_5^+ + 2HNO_2 \rightarrow \frac{3}{2} N_2 + 4H_2O + \frac{1}{2} H^+ \quad [16]$$

$$N_2H_5^+ + 3HNO_2 \rightarrow \frac{5}{2} N_2O + \frac{7}{2} H_2O + H^+ \quad [16a]$$

According to BIDDLE (33), reaction [15] is of the first order compared to hydrazine and nitrous acid. At 20° for the following concentrations (HNO_2 = 10^{-2} M, $N_2H^+_5$ = 0.1 M, HNO_3 = 2M) the half-reaction time of this reaction rises to $1.7 \cdot 10^{-3}$ s (33).

In the absence of hydrazine, nitrous acid and, therefore, N_2O_4 ($N_2O_4 + H_2O \uparrow HNO_3 + HNO_2$) as well, oxidizes Pu(III) by self-catalysis according to the following equation (22):

$$2Pu^{3+} + 2HNO_2 + HNO_3 + 2H^+ \rightarrow 2Pu^{4+} + 3HNO_2 + H_2O \quad [17]$$

Measurements of the kinetics lead to the following equation of rate:

$$\frac{d\,|Pu(III)|}{dt} = -k\,|Pu(III)|\,|HNO_2|\,|H^+|\,|NO_3^-| \quad [18]$$

An activation energy of 58.6 kJ.Mol^{-1} has been determined. The constant k at 20°C is 60 (Mol.l^{-1})$^{-3}$.min^{-1}. However, for nitric acid concentrations below 0.4 Ml^{-1} (pH > 0.3), nitrous acid no longer works as an oxidant of PU(III) (34, 35), but, on the contrary, reduces PU(IV) although slowly, as shown by the Pourbaix diagrams given in Appendix II (figures AII-1). The oxidation of U(IV)

by nitrous acid evolves much more slowly than that of Pu(III) (36), but is is catalyzed by Pu.

In the organic phase as well, the oxidation of Pu(III) takes place in the presence of the nitrite ion, as shown by polarographic and spectrophotometric measurements (31, 37). The reoxidation of Pu(III) will be treated in detail in Chapter II (section II - 5) because it is of primary importance to an understanding of the reactions in the mixer-decanter.

I - 2.4. Hydrazine

The standard potential is - 0.23 V (ESH) for the pair:

$$N_2 + 5H^+ + 4e^- \rightleftharpoons N_2H^+_5 \qquad [19]$$

As was to be expected, hydrazine is oxidized before Pu(III) at a Pt anode because of this. However, high overvoltages of approximately 900 mV (26) are observed.

Hydrazine reduces Pu(IV) to Pu(III) fairly slowly, slower than Fe(II) and U(IV). This is surprising from the thermodynamic standpoint because of the large difference of standard potentials. According to KOLTUNOV (38), the reduction takes place is several stages:

$$Pu^{4+} + H_2O \rightarrow Pu(OH)^{3+} + H^+$$

$$Pu(OH)^{3+} + N_2H^+_5 \rightarrow Pu^{3+} + N_2H_3 + H^+ + H_2O \text{ (slow)} \quad [20]$$

The hydrazyl radical can then reduce Pu^{4+} according to the following:

$$N_2H_3^- + 3Pu^{4+} \rightarrow N_2 + 3PU^{3+} + 3H^+ \quad \text{(quick)}$$

or be dismuted into ammoniac and nitrogen:

$$2N_2H_3 + N_4H_6 \rightarrow 2NH_3 + N_2$$

In fact, two reaction processes are observed:

$$2Pu^{4+} + 2N_2H^+_5 \rightarrow 2Pu^{3+} + 2NH^+_4 + N_2 + 2H^+ \quad [21]$$

$$4Pu^{4+} + N_2H^+_5 \rightarrow 4Pu^{3+} + N_2 + 5H^+ \quad [22]$$

Reaction [21] is promoted by a high hydrazine concentration, reaction [22] by a lower concentration. Assuming $Pu(OH)^{3+}$ and $N_2N^+_5$ as reactive species, KOLTUNOV obtains the following reaction rate equation:

$$\frac{d\,|Pu(IV)|_s}{dt} = k\,\frac{|Pu(IV)|\,|N_2H_5NO_3|}{(K_{HP} + |H^+|)} \quad [23]$$

and an activation energy of 92 kJ.Mol.l^{-1}. At 20° K is 0.011 min^{-1}.

CHAPTER II

EXPERIMENTAL STUDY OF THE PROCESS INVOLVED IN AN ELECTROREDUCTION MIXER-SETTLER

In this chapter we our presenting our research on the corrosion of the electrodes and the kinetics of the oxidation-reduction reactions.

II - 1. Corrosion Research for Materials Selection

II - 1.1. Cathode Selection

In order to orient the selection of the cathode material, in addition to the electrochemical reduction efficiencies, we studied the usual rate of electrode corrosion in a typical electrolyte of the PUREX process (1 M HNO_2, 0.2 M $N_2H_5NO_3$, 0.1 M U, 0.02 M Pu, saturated by 20% volume of TBP/dodecane) for a cathode current density of 25 $mA.cm^{-2}$. (Table 1), (26)

Thinning rates were determined by measurement of the weight loss of the electrodes. Table 1 given the results obtained. We see that titanium has a very slow corrosion rate (0.2 mm/yr). Since it also produces good electrochemical results, it was preferred to platinum, tantalus and hafnium for reasons of price and availability.

Table 1: Measurements of cathode thinning

Corrosion rates of various materials

Electrolyte: [the rest of the table is illegible]

[illegible]

[illegible]	[illegible]	
	[illegible]	[illegible]
[illegible]	[illegible]	[illegible]
[illegible]	[illegible]	[illegible]
[illegible]	[illegible]	[illegible]
[illegible]	[illegible]	[illegible]
[illegible]	[illegible]	[illegible]
[illegible]	[illegible]	[illegible]
[illegible]	[illegible]	[illegible]
[illegible]	[illegible]	[illegible]
[illegible]	[illegible]	[illegible]

Measurement of anode thinning

Corrosion rates of various materials

Electrolyte: [the rest of the table is illegible]

[illegible]

[illegible]	[illegible]	
	[illegible]	[illegible]
[illegible]	[illegible]	[illegible]
[illegible]	[illegible]	[illegible]
[illegible]	[illegible]	[illegible]
[illegible]	[illegible]	[illegible]
[illegible]	[illegible]	[illegible]
[illegible]	[illegible]	[illegible]
[illegible]	[illegible]	
[illegible]		
[illegible]		

Recent corrosion tests of titanium under cathode polarization performed in an electrolyte constituted of HNO_3 2.5 M and $N_2H_5NO_3$ 0.2 M convinced us that corrosion increases with the current density and decreases by one order of magnitude in the presence of uranyl ions at a concentration of 0.1 $M.l^{-1}$ (Table 2), (39).

Table 2: Corrosion Rate of titanium

2.5 M NHO_3, 0.2 M $N_2H_5NO_3$, T = 25°C

mA/cm²	Thinning	
	without $UO_2$2+	with $UO_2$2+ (0.1 M/l)
5	0.34	0.022
15		0.088
50	0.67	0.018[?]

In addition to the corrosion of titanium itself, its embrittlement by hydrogen with possible formation of hydride must be taken into account. This fixation of hydrogen by a titanium cathode was examined for a current density of 10 $mA.cm^{-2}$ in an ele4ctrolyte containing HNO_3 1M, $N_2H_5NO_3$ 0.1 M, $UO_2$2+ 0.1 M. Even after 2800 hours of operation, it was possible to find only 0.003% hydrogen by weight (39). Likewise, tests of the fatigue strength of titanium sheets subjected to the same conditions showed no difference with untreated specimens. Therefore, titanium embrittlement is obviously not to be feared under our experimental conditions.

A considerable decrease of the corrosion rate is possible by the use of a titanium alloy with 0.2% palladium. In an electrolyte free of uranyl ions, the corrosion rates are ten times smaller for this alloy than for pure Ti (39).

II - 1.2. Anode Selection

For the anode there can be no question of anything other than noble metals since, under these conditions, all the other metals dissolve easily or their surfaces are covered with a passivation layer (Table 1). (26). Gold appears to have good resistance to nitric acid but the surface layer of oxide that is formed can be easily detached mechanically and it also dissolves in hot nitric acid. Therefore, for use in the PUREX process, platinum or a platinum plated substrate such as titanium or tantalus are the only materials with a sufficiently low corrosion rate. We have noted (figure 3) that the corrosion rate of platinum increases almost linearly with current density. It also increases with temperature. These results are in agreement with those of CARRACCIOLO (40). The latter also observed an increase of corrosion when the nitric acid concentration was decreased.

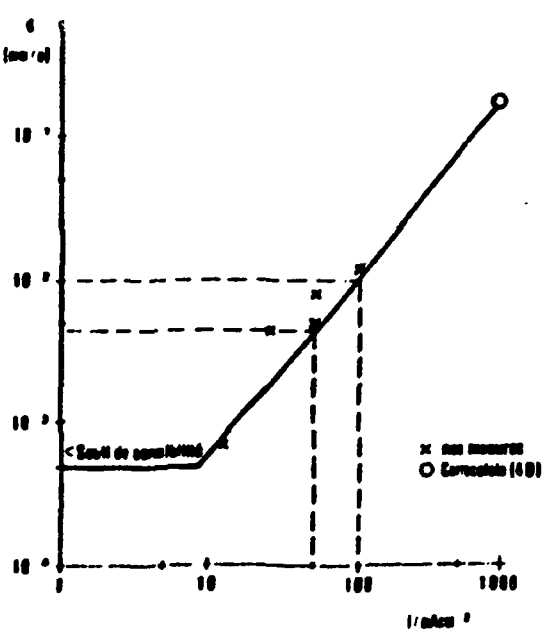

Figure 3: Corrosion of platinum as a function of current density

Electrolyte: $HNO_3 - N_2H_5NO_3$

In an electrolyte containing HNO_3 0.4 - 2.5 M and $N_2H_5NO_3$ 0.2 M, the corrosion rates of Pt determined by weight loss are within the limits of detection of $5 \cdot 10^{-4}$ mm per year for a current density of 12 $mA.cm^{-2}$. Even for 100 $mA.cm^{-2}$, the thinning only reaches $1 \cdot 10^{-2}$ mm per year. The presence of uranyl ions slightly reduces the corrosive effect (39). By adopting an anode current density of 50 - 100 $mA.cm^{-2}$ for the reprocessing plant facility, we have to deal with an annual anode thinning due to corrosion of 5 to $10 \cdot 10^{-3}$ mm.

For financial reasons, solid platinum anodes cannot be used. In industry, platinum-plated supports will be used. To this category belong the group IVa and Va metals which have the advantage of being passivated under anode polarization if the efficiency is partially distroyed.

Until now the majority of experiments has been performed with tantalus electrodes covered by electrolysis in a bath of melted salts with a platinum film. The corrosion rates for platinum plated electrodes prepared by this method are identical to the rates obtained for sheets of solid platinum.

Titanium can also be used as a support. However, its breakdown voltage of 10 V is relatively low, which limits its use.

II - 1.3. Insulating Material

The selection of insulation is limited. Due to radiation, the use of synthetic materials poses problems and was only done during tests. In the industrial facilities, we use an aluminum oxide ceramic sintered at very high temperature which is very resistant to chemicals and to radiation.

II - 2. Electroreduction of Pu(IV)

II - 2.1. Electrochemical Study

In order to understand the phenomena of electroreduction in the mixer-settler better, we studied the limiting current densities on fixed platinum and titanium cathodes by voltammetry in a solution of nitric acid containing Pu(IV) (41). The schematic drawing of the experimental facility is shown in figure 4a.

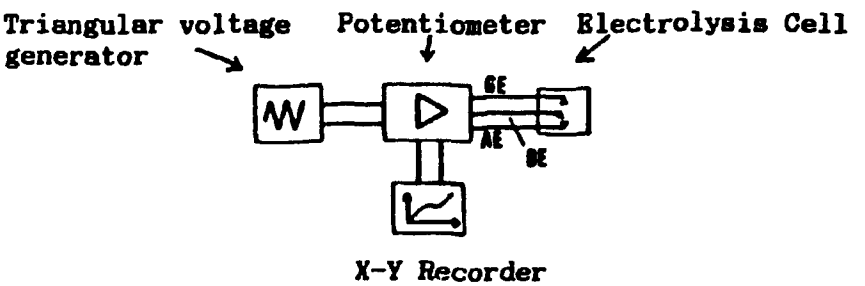

Figure 4a: Experimental setup for cyclical voltammetry

Compared to the reference electrode (RE), the potential of the working electrode (AE) is regulated by controling the current density between this electrode and the counter-electrode (GE). A potentiostat controlled by a voltage generator setting the rate and amplitude of potential variations is used. By applying a periodic triangular voltage, we obtain cyclical voltampereograms representing the variations of the current on the anode and cathode directions.

As a measurement electrochemical cell, we used a thermostated beaker without diaphragm, shown in figure 4b.

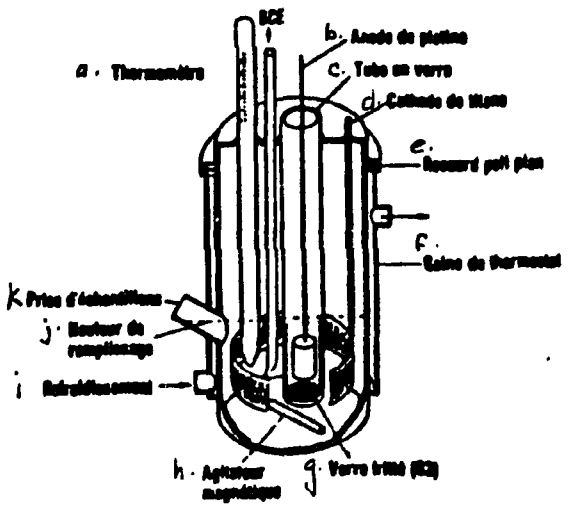

Key:
a. Thermometer
b. Pt anode
c. Glass tube
d. Ti cathode
e. Plane polished connector
f. Thermostat sheath
g. Sintered glass [illeg.]
h. Magnetic agitator
i. Cooling
j. Filling height
k. Sampling point

Fig. 4b: Test apparatus for the chemical and electrochemical reduction of Pu^{4+}

The experimental conditions are as follows:

Electrodes: Working electrode: Platinum or titanium blade

Counter-electrode: platinum blade

Reference electrode: ESC with HABER-LUGGIA capillary

Electrolyte: Composition: HNO_3 0.6 to 1.2 M

Pu^{4+} 0.05 to 0.3 M

Volume: 25 ml

Temperature: Approx. 25 to 35° C

Apparatus: Potentiostat: WENKING ST 72

Voltage generator: WENKING VSQ 72

X-y Recorder

Magnetic agitator (100 to 200 rpm)

The voltamperograms on the titanium and platinum electrodes have been recorded by varying the potential according to a triangualr program starting from a rest potential or from an OV potential for the cathode and going up to hydrogen liberation.

As a general rule, between 10 and 15 cycles are required before the voltamperogram obtained is stationary. The variation rate of the potential was determined in preliminary tests at 10 and 1 $mV.sec^{-1}$. It turned out that a variation of this sort practically did not change the appearance of the curve obtained. Therefore, we adapted a scan rate of 10 $mV.sec^{-1}$ for all the later experiments.

Finally, in order to obtain reproducible experiments, the electrodes where always cathodicly treated at I = 2A in HNO_3 1 M for an hour prior to each test.

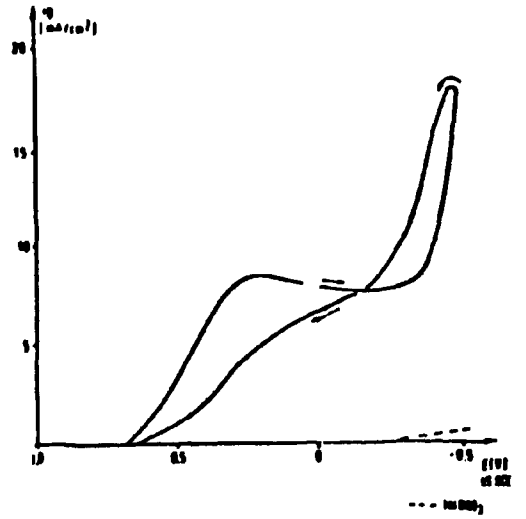

Figure 5: Density curve of current/potential, AE: Platinum
+780 ~ -500 mV; T = 21.5°C, 0.322 M Pu; 0.87 M HNO_3
[Trans. note: all of the above figures are subject to question, since the copy is almost illegible.]

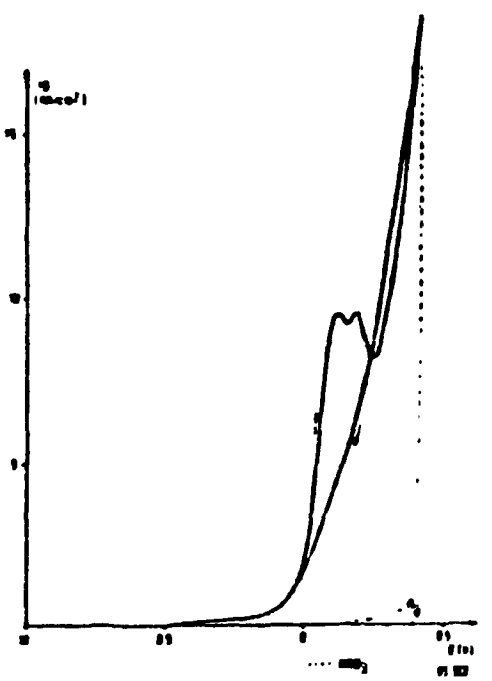

Figure 6: Density curve of current/potential. AE: Titanium
[numbers illegible]

Figures 5 and 6 present typical I - E curves. The curves drawn with a dotted line relative to a nitric acid solution show that the reduction of nitrates and of protons can be neglected. The intensity of the maximums, therefore, constitutes a direct measurement of the rate of reduction of Pu(IV). Both for the titanium and for the platinum, these curves show considerable overvoltages with their half-wave potential of 0.15 V for platinum and 0.7 V for titanium respectively compared to the standard hydrogen electrode (ESH).

In order to unite the experimental conditions and to reduce the measurement time, we set a scanning range of 0 to 300 mV (ESC) and allowed as limiting current densities the current densities establishing themselves around -200 mV. Figures 7 and 8 represent these densities as a function of the Pu(IV) concentration.

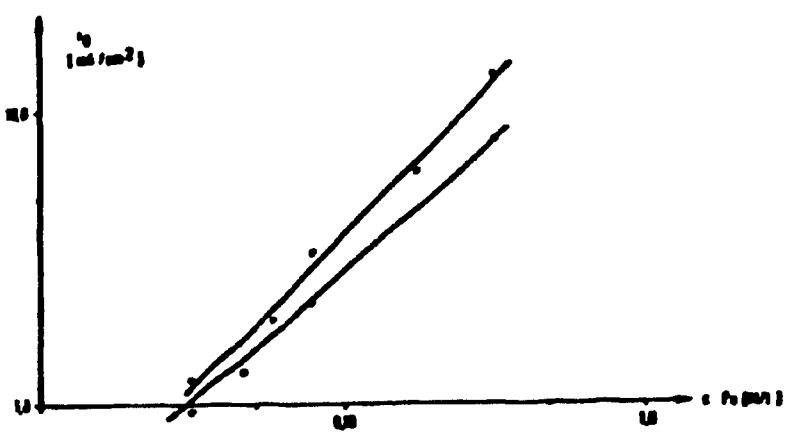

Figure 7: [illegible]

The almost linear appearance of the graphs reinforces the hypothesis of a rate law controlled by the transport of material. For a reaction of the first order

the transport constant β is related to the limiting intensity by the following relationship:

$$i_g = \beta \cdot zF.C \qquad [24]$$

(i_g = limit current density, z = electrochemical valence, F = Faraday constant, β = transport constant $cm.min^{-1}$, C = concentration).

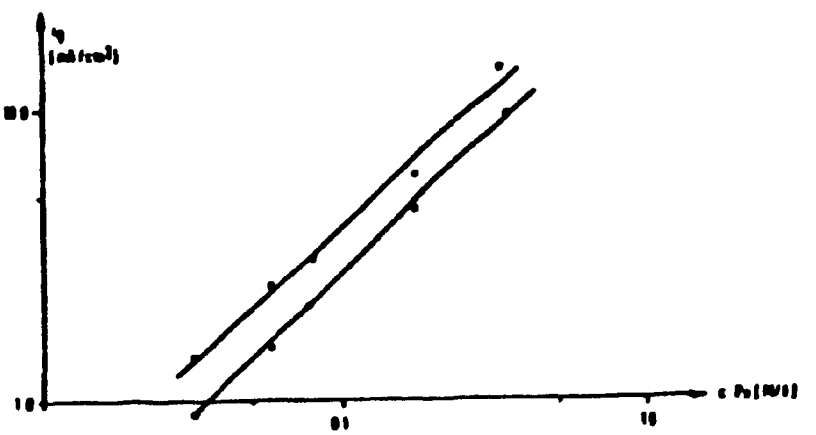

Figure 8: [illegible]

Table 3 gives the average limiting current densities for all the tests performed and the resulting transport constants for various temperatures of an agitated electrolyte (magnetic agitator, approx. 150 rpm) and at rest.

Cathode		T °C	Densité de courant limite moyenne mA/cm² 0.1 m Pu(IV)	Coefficient de transport β cm/min
Titane	[illegible]	22 ± 1 26 ± 0.5	3.4 4.7	0.021 ± 0.01 [illegible] ± 0.01
	[illegible]	22 ± 1 26 ± 0.5	[illegible] [illegible]	0.13 ± [illegible] 0.25 ± [illegible]
Platine	[illegible]	25 ± 1 [illegible]	3.4 4.2	0.021 ± [illegible] [illegible] ± [illegible]
	[illegible]	25 ± 1.2 [illegible]	27.3 37.8	0.17 ± [illegible] 0.23 ± [illegible]

[illegible]

Table 3: Limiting current densities and transport coefficients for Pu(IV) [illegible] solutions

At high concentrations of Pu(IV), the reproducibility of the measurements leaves something to be desired, which reflects the high value of the mean deviations. We note an influence of the temperature and the agitation. The large increase of β when the electrolyte is agitated is moreover the indication that the process is indeed determined by the transport (diffusion), which explains the small differences between the values of β found for platinum and titanium.

II - 2.2. Application to the case of the Mixer-Settler

Using the measured transport constants, we can estimate the direct portion of electroreduction during the reduction of Pu(IV) in the mixer-settler. In fact, in the latter, the agitation is less than in our tests. The average value of β is, therefore, probably between the two values measured for a non-agitated and an agitated electrolyte.

We assume that the fluid flow is of the piston type, that the solution is absolutely homogenous and that the transport constant β is independent of the concentration. The general equation of the material balance is then written as follows:

$$-Q.dC = \beta.\ \Omega\ .\ C.\ dl \qquad [25]$$

with C = flow, C = concentration, Ω = specific surface of the electrode per unit of length of the reactor ($cm^2.cm^{-1}$), l = length.

In case the average current density is above the limit current density ($i > i_g$) and uniformly distributed, the following law of rate is derived from it:

$$\frac{d\,|Pu(IV)|}{dl} = -\frac{\beta\,|Pu(IV)|}{Q} \qquad [26]$$

For a mixer without flow, this equation is written as follows:

$$\frac{d\,|Pu(IV)|}{dt} = -\beta\,\frac{O_K}{V}\,|Pu(IV)| \qquad [27]$$

(O_K = cathode surface, V = mixer volume)

It should also be noted that the rate equations are only valid in the acid range of 0.6 to 1.2 M where there are no variations of the reduction rate with the acid concentration.

II - 3. Electroreduction of U(VI)

We have studied the electroreduction of U(VI) on rotating platinum and titanium electrodes by cyclic voltametry (43). We have also found the reduction potentials given by (26) (half-wave potential: on Pt, approximately + 70 mV, on Ti, approximately -160 mV compared to the hydrogen electrode). We have also confirmed that the order of the reaction is practically equal to 1 compared to uranium. For platinum, the reduction current increases considerably with the rotation speed but it cannot be said that the process is controlled by transport since i_g is not a linear function of the square root of the rotation speed.

The voltameter measurements make it possible to formally estimate the transport constants for the electrolyte at rest. We find respectively for Pt and Ti a value of β to be $2 \cdot 10^{-2}$ cm.min^{-1} and $5 \cdot 10^{-4}$ cm.min^{-1}. This latter value must not, however, be considered as representative of the titanium cathodes used technically, since under our test conditions and for scanning rates above 10 mV.s^{-1}, the current densities reach their stationary value only after a relatively long time, as the efficiency measurements show (43).

The variation of the reduction rate as a function of the acid concentration was not examined. In the case of hydrochloric acid, the influence of the concentration is apparent only for concentrations below 0.3 M (44). In this acid, the activation energy of the U(VI) reduction obeys a law of rate of the first order compared to U(VI) and is 13 kJ.mol^{-1}. As for the electroreduction of Pu(IV), we shall therefore use the following equation of rate giving variation as a function of time of the concentration of U(VI) in the extractor:

$$\frac{d\,|U(VI)|}{dt} = -\beta \frac{O_K}{V}\,|U(VI)| \qquad [28]$$

For the numerical application of the model, the values of β are taken from the efficiency measurements in the simulation cells (26). They are average values evaluated from the integrated form of equation [28]. In the case of a stationary flow, we have:

$$\beta_m = \ln \frac{|U(VI)|_1}{|U(VI)|_2} \cdot \frac{Q}{O_K} \qquad [29]$$

Where β_m = average transport constant

index 1 = feed solution

index 2 = exiting solution containing the products

Q = flow rate

O_K = cathode surface

The transport constants vary greatly with the average current densities and depend on the geometry of the cells used (26). However, they are in good agreement with the efficiency measurements previously cited (43). All of the estimates of the reduction rates by this method are, of course, approximations, since as we said, we assume that the flow is of the piston type, simpler than the real hydrodynamic conditions and that the distribution of the current density is uniform.

II - 4. Reduction of Pu(IV) in the Presence of Hydrazine

During the counter-current extraction tests, it turned out that the mixer-settler installed in the Karlsruhe reprocessing plant (WAK) had a much greater hydrazine consumption than the lab prototype (46). Since these tests were performed for reduced flow rates, the average time the phases stayed in the apparatus was abnormally long, whence the hypothesis that hydrazine was consumed in the reaction with the nitrites (equation 15) formed during the reoxidation of the Pu(III) in the organic phase (equation 17). But, since we also found the NH^+_4 ion in the solutions of the Pu produced, it had to be assumed that $N_2H^+_5$ also acted according to equation 21. This reaction is all the more probable since the WAK mixer-settler has a smaller specific cathode surface that the lab apparatus. The result is that the reduction of Pu(IV) by hydrazine can compete with the electroreduction. In order to verify this hypothesis, we simulated the conditions of reduction of Pu(IV) by hydrazine suing a cell shown in figure 4b. We were able to show in this way that the reduction by hydrazine is catalyzed in the presence of the electrodes (45). This catalysis is due basically to the traces of platinum deposited on the titanium cathode by the corrosion of the anode. The magnitude of the catalytic effect depends on the temperature and the specific surface Ω of the cathode.

This research was pursued by HEILGEIST (46) who confirmed the validity of the rate equation proposed by KOLTUNOV (38) (equation 23) by the catalysed reaction:

$$\frac{d\,|Pu(IV)|}{dt} = -k^{*}\,\frac{|Pu(IV)|\;|N_2H_5^+|}{(k_{HP} + |H^+|)} \qquad [30]$$

where k* is the constant of the catalysed rate. The experiment shows that k* varies linearly with the specific cathode surface (Ω, cm^2, cm^{-3}).

$$k^* = k + m\Omega \qquad [31]$$

k being the constant of rate of the uncatalysed reaction. The coefficient m is 0.221 $cm.min^{-1}$ at 35° C. For an initial ratio $|N_2H^+{}_5|_o/|Pu(IV)|_o$ of 14, an activation energy of 92.2 $kJ.Mol^{-1}$ is calculated for the uncatalysed reaction and 27.2 $kJ.Mol^{-1}$ for the catalysed reaction (Ω = 0.52 $cm^2.cm^{-3}$). Up to a value of 5 for the ratio $|N_2H^+{}_5|/|Pu(IV)|_o$, the activation energy exhibits only slight variations. In addition, we note that it depends little on the ionic force (μ varying from 1 to 2) (38, 39). Table 4 contains the rate constants measured between 20 and 50°C as well as the hydrolysis constants k_{HP} for Pu(IV) taken from the literature.

Table 4: Rate Constants of the uncatalysed and catalysed reduction* of Pu(IV) with hydrazine

T, °C	Constante de vitesse (min⁻¹)		Constante d'hydrolyse de Pu (IV) (M/l)
	k	k'(Ω = 0.5)	k_{hyd}
20	0.011	0.08	0.048
25	0.021	0.12	0.054
30	0.038	0.14	0.068
35	0.073	0.18	0.082
40	0.148	0.25	0.094
45	0.237	0.40	0.11
50	0.370	0.60	0.13

II - 5. Self-catalysing oxidation of Pu(III) in the organic phase

The kinetics of the self-catalysing oxidation of Pu(III) have been studied in the aqueous phase by DUKES (22) who proposed the following mechanism with N_2O_4 as the reactive species:

$$HNO_2 + HNO_3 \rightleftharpoons N_2O_4 + H_2O \text{ (quick, reversible)} \quad [32]$$

$$N_2O_4 + Pu^{3+} \rightleftharpoons NO^-_2 + NO_2 + Pu^{4+} \text{ (slow, regulates the rate)} \quad [33]$$

The oxide N_2O_4 formed then reacts as follows:

$$NO_2 \rightleftharpoons 1/2\ N_2O_4 \quad [34]$$

$$N_2O_4 + H_2O \rightarrow HNO_2 + H^+ + NO^-_3 \quad [35]$$

The sum of these reactions represents the overall reaction [17]:

$$2Pu^{3+} + 2HNO_2 + NO^-_3 + 3H^+ \rightarrow 2Pu^{4+} + 3HNO_2 + H_2O$$

during which more HNO_2 is formed than is consumed (self-catalysis).

This reactions was also observed in the organic phase (31, 37, 47). Spectrophotometric measurements show a sigmoid evolution of the concentration |Pu(IV)| as a function of time, which confirms the self-catalysis (37, 47) and shows that over time the ratio $|HNO_2|_t$ / $|Pu(IV)|_t$ remains constant and equal to 0.5, in agreement with the overall equation [17] (37).

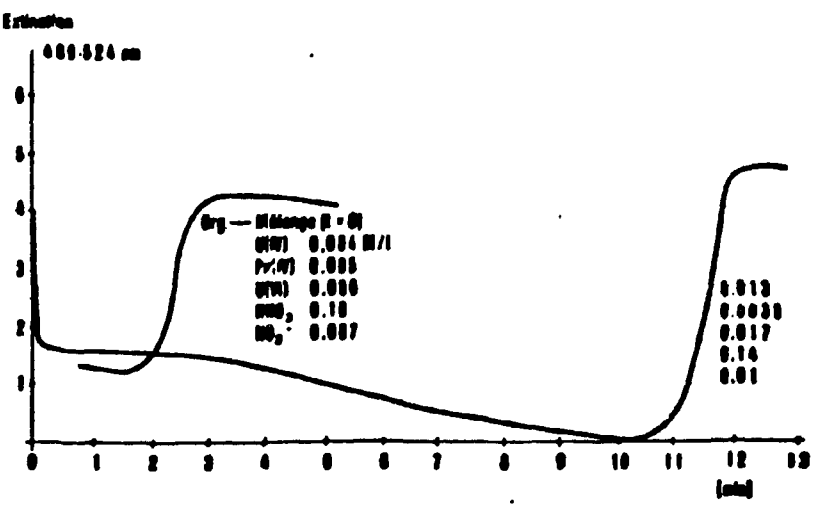

Figure 9: Evolution of the oxidation of Pu(III) and U(IV) in a 30 % Vol. solution of TBP at 30% V at room temperature

Figure 9 gives our own results about the degree of advancement of the reaction of the two mixtures at room temperature in solution in TBP at 30%V (47). In each case, we start with organic solutions of TBP containing Pu(IV) and U(IV).

The approximate compositions of two of these solutions at the initial instant are given in figure 9. They are mixed directly in the cup of the spectrophotometer and the quenching at 489 mm is followed for a certain time. At this wave length, Pu(IV) has an absorption maximum covered by a band of U(IV). Knowing the specific quenching coefficients in the organic phase, it it then possible to calculate the concentrations of each component (48). These results, however, are only indications, since the analysis method used must be improved.

The polarographic study of the oxidation of Pu(III) in organic phase brought BIDDLE (31) to a rate law of the following form:

$$-\frac{d\,|Pu(III)|}{dt} = \frac{d\,|Pu(IV)|}{dt} = k^{*}\,|Pu(III)|\,|N_2O_4| \qquad [36]$$

where it is assumed that N_2O_4 is the active species. Since the equilibrium between HNO_2 and N_2H_4 (equation 32) must probably be reached as quickly in the organic phase as in the aqueous phase, the concentration $|N_2O_4|$ is proportional to $|N+HNO_2|$. On the other hand, the rate constant varies as a function of the nitric acid concentration of the organic phase. Analysis of BIDDLE's results obtained at 20°C showed that the function $k^* = f(|HNO_3|_o)$ can be written in the empirical form:

$$k^* = \exp(7.28\,|HNO_3| + 5.83) \qquad [37]$$

Therefore, it can be seen that the experimental oxidation rate of Pu(III) in the organic phase is really proportional to $|HNO_2|$ and $|Pu(III)|$ but depends on the HNO_3 concentration in a different way than indicated by formula [18] in the aqueous phase.

In the presence of U(IV) in the organic phase, we should expect the intervention of two paired processes: oxidation of Pu(III) by HNO_2 and the reduction of Pu(IV) by U(IV) ending up with the complete oxidation of Pu(III) and U(IV):

$$2Pu^{3+} + 2HNO_2 + NO_3^- + 3H^+ \rightarrow 2Pu^{4+} + 3HNO_2 + H_2O \qquad [38]\ (*)$$

$$2Pu^{4+} + U^{4+} + 2H_2O \rightarrow 2Pu^{3+} + UO_2^{2+} + 4H^+$$

The oxidation rate of Pu(III) resulting from these paired processes is then written as follows, accounting for reactions [36] and [8b]:

$$\frac{d|Pu(IV)|}{dt} = k^* |Pu(III)||NO_2^-| - k \frac{|Pu(IV)||U(IV)|}{(|H^+| + 0.05)^2} \qquad [39]$$

---

* NOTE: This reaction loop explains the "accelerated oxidation of U(IV) in the organic phase in the presence of plutonium" frequently cited in the literature. In the absence of plutonium, U(IV) is in fact oxidized much more slowly (36) and the rate is very sensitive to the presence of oxygen, among other factors (49).

From this equation, and accounting for the stoichiometry of the reaction [38], the evolution of a mixture of solutions corresponding to case 1 of 1a, figure 9 was simulated by numerical approximation. The result is shown in figure 10b and shows that the oxidation is complete after 7 minutes for k = 0.5 and 5 min for k = 1.

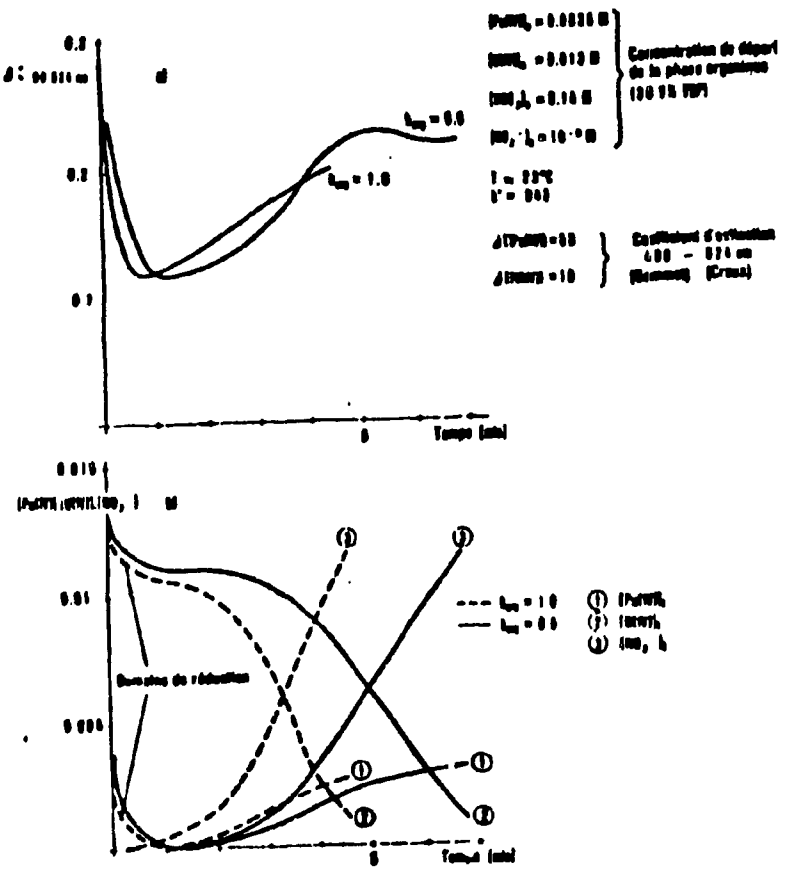

Figure 10: Simulation of self-catalysing oxidation of Pu(III) in an organic solution (30%V TBP) in the presence of U(IV)

[illegible]

Although these times are shorter than the experimental values, the characteristic appearance is well rendered, as shown by figure 10a in which the Pu(III) and U(IV) concentrations have been converted to quenching at 490 nm, which allows a direct comparison with figure 9.

The above results very probably give the explanation of the large excesses of U(IV)[4] which are necessary in practice for the separation of U/Pu when external U(IV) is used as the reducing agent (36, 50). In fact, since it is not abnormal for the separated organic phase to stay several minutes in the settler portion of the apparatus, it should be expected that a portion of the U(IV) extracted be reoxidized.

[4]The necessity of these excesses is surprising from the thermodynamic standpoint (see Appendix III).

CHAPTER III

STRUCTURE AND OPERATION OF AN ELECTROREDUCTION MIXER-SETTLER

III - 1. Design of an Electroreduction Mixer-Settler

As we said, our corrosion research and efficiency measurements have led us to select titanium as the cathode material. Then it is natural to make the entire apparatus of titanium and to connect it to the negative pole in order to avoid possible corrosion of the intermediate conductors.

For technical reasons, we had to abandon the initial project of doing the reduction in the mixer itself, which would have made it possible to attain optimal efficiency of the electroreduction of Pu(IV) controlled by the transfer of material. In fact, on the one hand, introducing the anode into the mixer chamber considerably disturbs the contact of the phases and, on the other hand, it leads to breaks in the current when the organic phase constitutes the continuous phase instead of the aqueous phase, a case that is not always to be excluded under the practical conditions of operation. That is why we have placed the anode in the settler and that is where the reduction will take place. Reduction efficiency obtained in this way was sufficient (see Appendix IV).

The use of a diaphragm, which it is desirable to avoid for practical reasons (risks of breakage and clogging up), is not necessary. The experiments previously described have in fact demonstrated that the anode oxidation of hydra-

zine is promoted compared to that of Pu(III) and that (the oxidation) of U(IV) requires high overvoltages.

On the other hand, in mixer-settlers, high cathode/anode surface ratios are easily reached that make it possible to reduce the reoxidation of Pu(III) and U(IV). We selected an electrical current supply rather than a constant potential supply for technical reasons, because no reference electrode is reliable under the severe operating conditions of our apparatus. The higher current consumption due to operating at constant current is not a financial drawback because electricity costs represent only a very small part of the total reprocessing cost. Because of the lack of homogeneity of the current densities at the periphery of the anode, we must expect to have to use more negative potentials than those at which the reactions take place normally, which provokes the liberation of hydrogen, but the formation of this gas can be reduced empirically. Moreover, there is no risk of explosion due to hydrogen because the device is constantly ventilated in order to carry off the radiolysis gases.

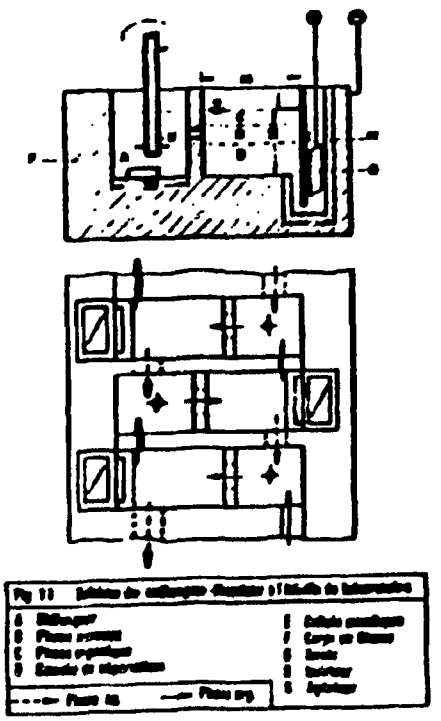

Figure 11 shows schematically the electroreduction mixer-settler on the laboratory scale (MILLI-EMMA) designed for a capacity of approximately 1 kg of fuel per day. The device installed in the Karlsruhe reprocessing plant (WAK-EMMA) for the second plutonium cycle has the same structure. The anode cell made of insulating material is located at a level below that of the mixer-settler. An opening at the bottom of the partition separating the anode compartment established the contact between the electrodes. This partition also acts as a separator, preventing the organic phase from penetrating the anode space, for example in case of breakdown when the organic phase completely pushes the aqueous phase out of the settler.

Table 5 summarizes the principle characteristics of the devices.

Table 5: [illegible]

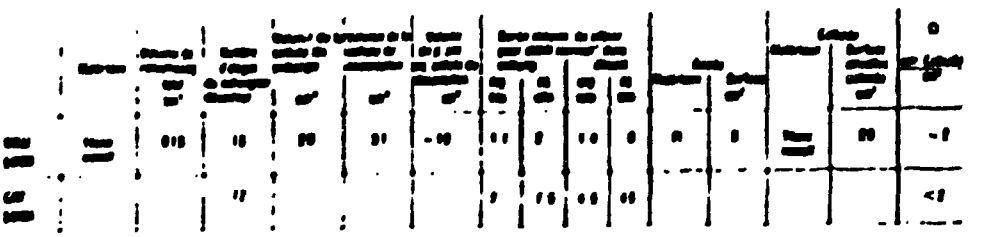

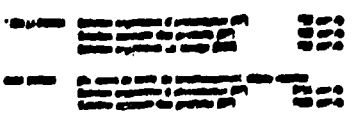

The titanium body of the laboratory device (MILLI-EMMA) is made of a single block and connected to the negative pole. The anode cells are plexiglas while, in the industrial mixer-settler (WAK-EMMA) they are made of ceramic material. For the MILLI-EMMA anode, a platinum plate with an effective surface per stage of 8 cm^2 was used. The agitators are driven via a common mechanism.

The laboratory device has 16 separation stages. In fact, efficiency test of extraction with uranium have revealed an efficiency by state that is clearly insufficient (26), which is not abnormal for a small extractor. Under these conditions, 16 stages are required to achieve the efficiency desired. On the other hand, the larger WAK extractor is equipped with only 12 stages.

In the case of plutonium processing, the mixer-settler is placed in a glove box equipped with the necessary apparatus (dosage pumps and graduated burettes) and, for all of the experiments, has been connected to the MILLI facility which allows supply of organic products (organic feed solution, AP) and the reextraction of the uranium present in the organic phase coming out of the electroreduction mixer-settler.

During the experimental phase, we used a total of 12 anode cells that could be placed in a variable way in the 16 settling chambers of the apparatus. The anode cells are individually supplied with constant current. In order to determine the cathode potential, we introduced titanium wires in the center of each settling compartment. In principle, these wires play the role of a comparison electrode. The potential values measured show, however, large fluctuations after only 200 hours of service and have only a rough indicative value.

Figure 12 shows the photo of the laboratory mixer-settler. On the top you can see the motor, the common drive device, the passage of the various agitators, the titanium body itself of the device and, finally, the settling chambers.

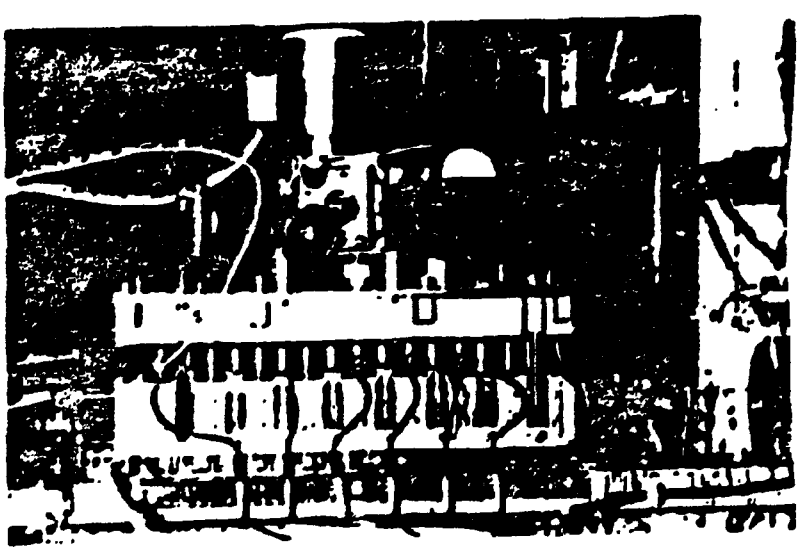

Fig. 12

III - 2. Selection of the Flow Chart for Counter-Current Extraction

III - 2.2. Pu Separation

Figure 13 shows the flow chart of U/Pu separation with a 16 stage mixer-settler.

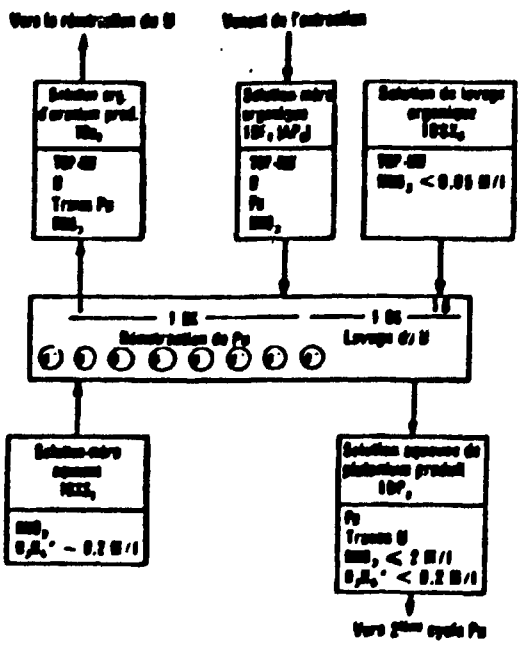

Figure 13: Flow chart of U/Pu Separation with the electroreduction mixer-settler in the first extraction cycle.
[illegible]

The abbreviations used to designate the various flows are part of a code introduced for reprocessing which will henceforth be applied for reasons of concision (see table of Abbreviations p. 94)

The organic feed solution of mother solution 1BF containing U and Pu exiting extraction after washing of fission products is introduced at the middle of the extractor. For the laboratory mixer-settler, this feed point is designed between compartments 7 and 11. The extractor is thus divided in half: the section for plutonium reextraction, 1BX, and the uranium washing section, 1BS. While the plutonium is extracted again in the feed aqueous phase 1BXS in 1BX, the organic washing solution, 1BSX, is used to extract the uranium still contained in the aqueous solution of plutoniium produced, 1BP. By a judicious choice of the flux ratios 1BF/1BX and 1BSX/1BXS, a good dose of the reducing agent the the optimal adjustment of the nitric acid concentration, the separation of the plutonium and uranium is achieved in the extractor. The concentration profile of the nitric acid is set by the concentration in 1BXS but also by the flux ratios 1BF/1BXS because the flux 1BF coming from the washing of the fission products carries approximately 0.1 to 0.2 M of nitric acid. In the compartment 1BX, the nitric acid concentration should be held as low as possible for two reasons. First, because the reextraction of Pu(IV) is promoted in that way and, second, because the speed of reduction of Pu(IV) by U(IV) varies as the inverse of the square of the nitric acid concentration (equation 5). On the other hand, a high concentration of nitric acid is required in 1BS to facilitate the extraction of the uranium. The latter is obviously reinforced by the increase of the flux ratio 1BSX/1BXS.

Hydrazine, a stabilizing agent, is introduced into the flow BXS. A concentration from 0.1 to 0.2 M is sufficient as shown by previous experiments performed with U(IV) as the reducing agent (36).

For the plutonium produced in 1BP, we try to reach the highest concentration possible. It is determined by the ratio of flows 1BF/1BXS. Since the reducing reextraction takes place in the 1BX portion, the anode cells have been placed in the settling chambers 1 to 12, during the counter-current tests.

III - 2.2. Reextraction of Plutonium in the Second Pu Cycle

The plutonium produced in the first extraction cycle is extracted after oxidation in the second Pu cycle from which the fission products have been removed by washing and reextracted under reducing conditions. The difference with the reducing reextraction of the first cycle is due to the fact that the uranium content is much lower. For a decontamination factor (DF) for uranium of 1000 in the first cycle, the proportion of uranium in the plutonium, for a light water reactor, is now only 10%.

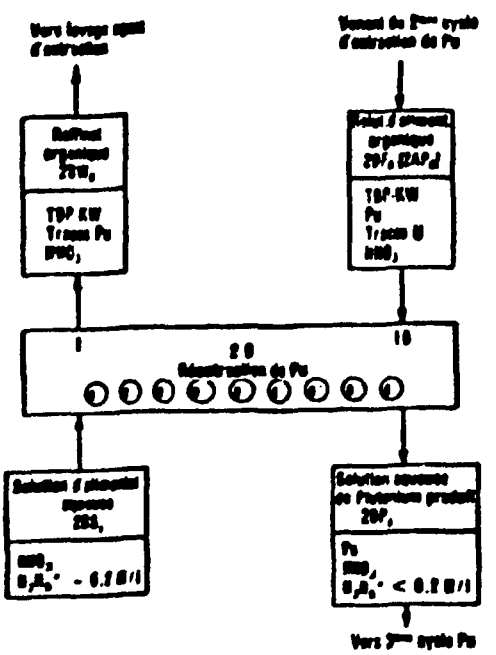

Figure 14: Flow chart of Pu reextraction with the electroreduction mixer-settler in the second Pu cycle

[illegible]

The flow chart for reextraction in the second cycle is shown on figure 14. The criteria set for the first cycle remain basically valid for the selection of the operating design. Since a later separation of the uranium is no longer essential, we can get along without the BS portion. In the laboratory extractor, the 16 stages can thus be used for reextraction. And for that reason, we can keep the nitric acid concentration as low as possible all along the extractor in order to increase the efficiency of reextraction. The electrochemical activity must happen in all of the compartments, which is the case with the 12 stage WAK mixer-settler.

III - 3. Results of Counter-Current Tests

III - 3.1. U/Pu Separation (U/Pu >> 1)

All of the tests were performed with 30% volume of TBP. The dilutant used is composed primarily of kerosene and n-dodecane (approximately 80% hydrocarbons in C11 + C12), with the fraction of isomers reaching some 2.5% vol.

The plutonium used in our laboratory tests had an isotope 239 content of 90% by mass. For the experiments with the WAK mixer-settler, we used a light water reactor fuel with a high fuel content with only about 67% mass of Pu-239 and 0.28% of Pu-238 (Pu-240: 26%, 241: 5%; 242: 1.7%).

The organic feed solution had an average Pu concentration of 0.66% by mass, a value that is characteristic for a light water reactor fuel with a low burnup rate.

The analytical methods for determining the oxidation states and concentrations for U and Pu, as well as the quantitative methods for nitric acid and hydrazine have been published in the literature (52,48). The absorption spectra of each oxidation state of Pu and U are shown in Appendix V. The minimum duration of a test in the mixer-settler is 13.5 hours. The uranium balance shows an average error of± 3% in our various tests.

The temperature of the aqueous and organic phases (1BU and 1BP) stayed below 35°C for an ambient temperature of 24°C. The temperature rise is cause in the first place by the heat released at the electrodes, and also by the friction heat of the drive system of the mixer-settler.

The nitric acid concentration in the aqueous feed solution 1BXS destined for Pu reextraction has always been set at 0.2 to 0.26 M. The hydrazine nitrate concentration of 0.2 M also remains constant in all of our tests. The rotation speed of the agitators varied between 1000 and 1100 rpm. An increase in the speed beyond 1100 rps is not hydrodynamically possible since the level of the aqueous phase in the settling chamber then drops too low (<20% of the volume of total filling).

The organic solution flow BSX was adjusted in each experiment in order to obtain a constant flow ratio 1BSX/1BF = 0.2.

The average voltage required reaches 2.8 V for 50 mA and 8.1 V for 300 mA.

For the rotation speeds used and for the flux ratios 1BF/1BXS between 7.1 and 9.3, the mixer-settler exhibited an average extraction efficiency, which is normal for a reduced scale device.

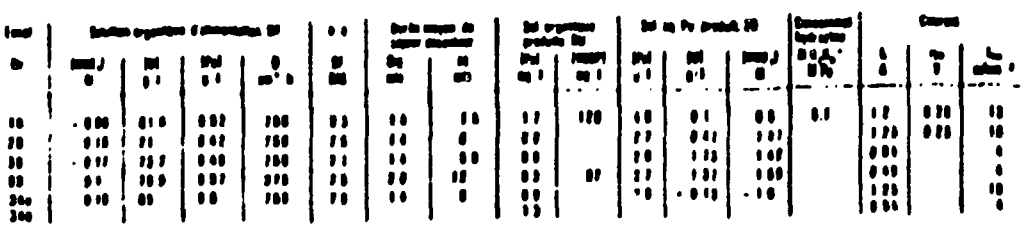

Table 6: Results obtained with the laboratory electroreduction mixer-settler [illegible] for U/Pu separation
[illegible]

Table 6 shows the results of six different experiments. In addition to the composition of feed and product solutions, it contains the average times in the process, the total current I_t, the overvoltage j_i measured by the titanium probe and the maximum average current density I_{max}. The total current results from the sum of the partial current intensities of all the settling chambers. We have generally equipped 8 settling chambers in compartment 1BX with anode cells.

Figures 15 and 16 show the concentration profiles obtained in tests 14 and 33. The partial current intensities were adapted to the quantities of uranium and plutonium to be reduced, as the figures show. For all of these experiments, the point of introduction of the organic solution 1BF was in chamber 9 except for test 33 where the introduction was done into compartment 11, so that there were only 5 compartments for the 1BS part.

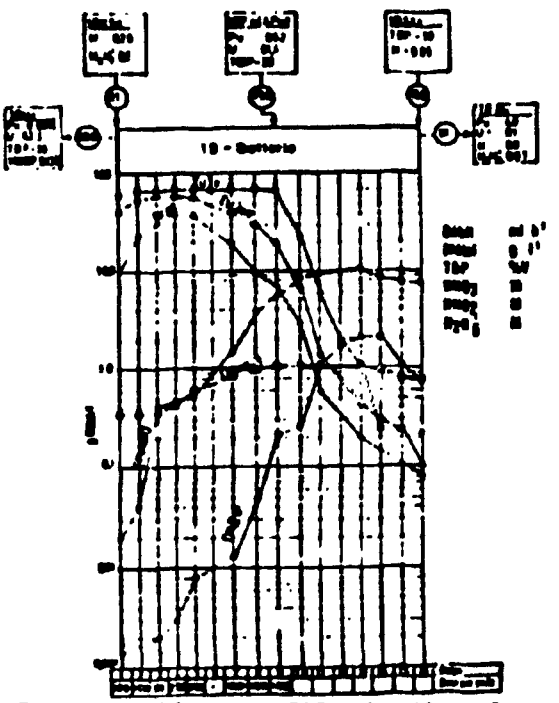

Figure 15: Concentration profile in the electroreduction mixer-settler [illeg.], Test No. 14.

The average maximum current density was estimated from the cathode surface given in table 5 and from the maximum partial current intensity. This value represents only an order of magnitude, because the distribution of the current density is certainly not homogeneous for the geometry of the mixer-settler. Likewise, the overvoltages measured using titanium wires introduced into the settling chambers must be considered as only approximate, because the titanium probe does not constitute a true reference electrode.

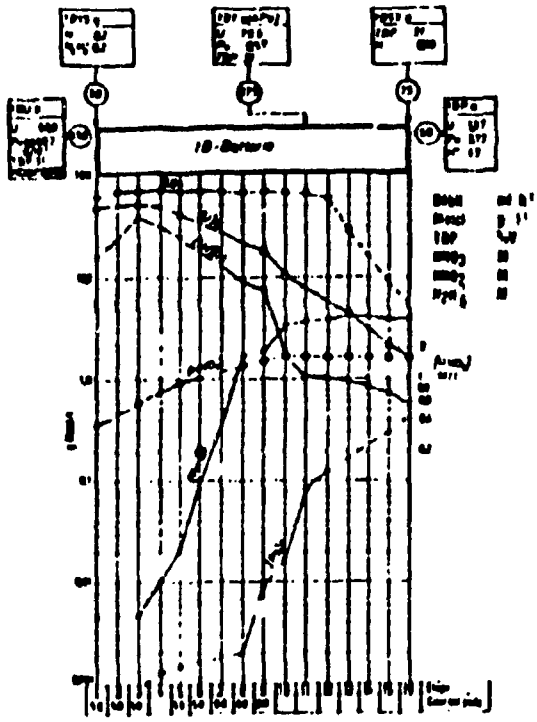

Figure 16: Concentration Profile in the Electroreduction mixer-settler [illegible], Test No. 33.

III - 3.2. Plutonium Reextraction (U/Pu < 1)

III - 3.2.1. Laboratory Mixer-Settler (MILLI-EMMA)

Given the fact that a later separation of the uranium in a part BS is not required here, the experiments were performed with the 16 stages of the mixer-settler used for the reextraction. For all of the experiments, the flow of the organic feed phase, 2BF, was held constant at the value of 0.2 l/hr.

Likewise, the composition of the aqueous feed solution, 2BS) remains identical (0.2 M $N_2H_6NO_3$ and 0.2 M HNO_3). The execution time of a single experiment was a minimum of 12 hours (test 18), but on the average, more than 20 hours. The temperature of the products never exceeded 33°C. The minimum voltage per cell, variable with the partial current intensity used, reached values of 3.6 V (test no. 18) to 6 V (test No. 30a). A rise in the rotation speed beyond 1100 rpm was impossible for the hydrodynamic reasons given below abourt U/Pu separation tests.

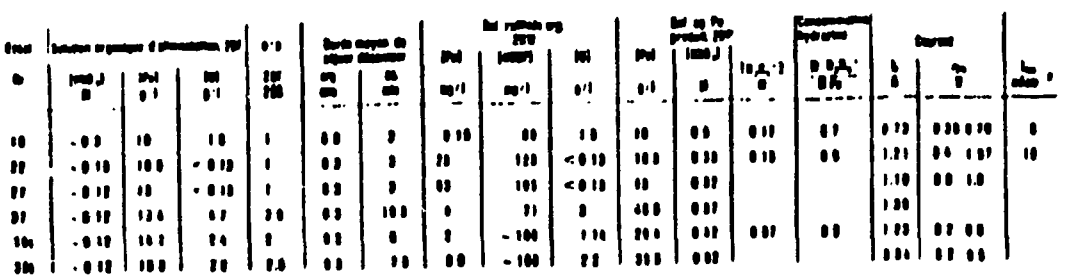

Table 7: Results obtained with the laboratory electroreduction mixer-settler (MILLI-EMMA) for the reextraction of Pu.

Table 7 shows the results of six experiments. The basic difference with the U/Pu separation experiments consists of the concentration of the organic feed solution 2BF, on the one hand, which is 30 to 40 times higher in Pu and 1000 times lower in U and, on the other hand, of the smaller flow ratio 2BF/2BF, reaching a maximum value of 3.5. The distribution of the total current among each settling cell was also set by the quantity of plutonium to reduce, as the concentration profile in figure 17 shows.

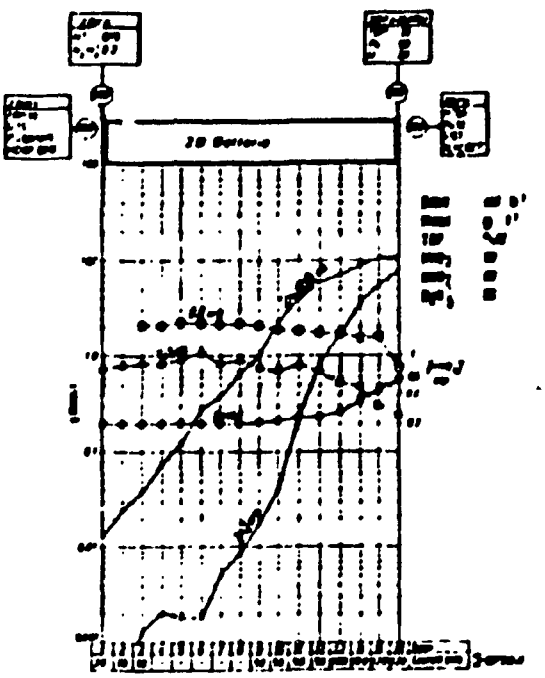

Figure 17: Concentration profile during Pu reextraction, Test No. 18

In principle, it is the settling chambers 1 and 3 and chambers 9 to 16 that were supplied with current. The supply of chambers 1 to 3 allows reduction of the remaining uranium to U(IV) in order to reextract more efficiently the Pu(IV) linked to the dibutyl phosphate (HDBP) (53). In order to show the influence of this complexer better, high concentrations were used (see Table 7).

III - 3.2.2. Industrial Mixer-Settler (WAK-EMMA)

The industrial mixer-settler is designed for a daily capacity of approximately 100 kg of light water reactor fuel, which is the equivalent of a quantity of 1 kg Pu produced per day. Note that, given the better extraction efficiency, only 12 cells were installed. The mixer-settler is differentiated from the laboratory one by its smaller specific cathode surface. For technical reasons, the facility operated during the tests only with greatly reduced flow rates, corresponding to long process times, more specifically for the aqueous phase, as shown by Table 8 where the results obtained are listed.

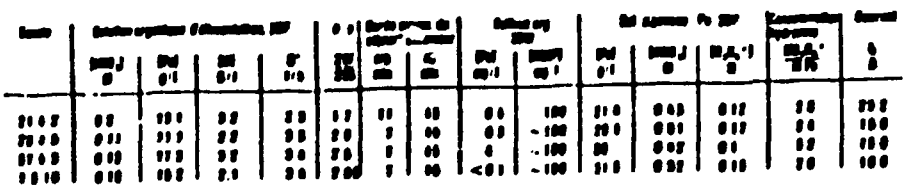

Table 8: Results of tests of the WAK industrial electroreduction mixer-settler [WAK-EMMA] for the reextraction of Pu (second cycle of Pu).
[illegible]

In 2BS, the nitric acid was maintained almost constantly at the concentration of 0.1 M, while that of the hydrazine varied between 0.35 and 0.65 M, or considerably above the values selected for the laboratory mixer-settler. Because of the longer staying times, the solutions got much hotter than in the lab apparatus. In the aqueous solution of products and in the organic phase, temperatures of 35° - 45° C and of 34° - 38° C respectively were recorded.

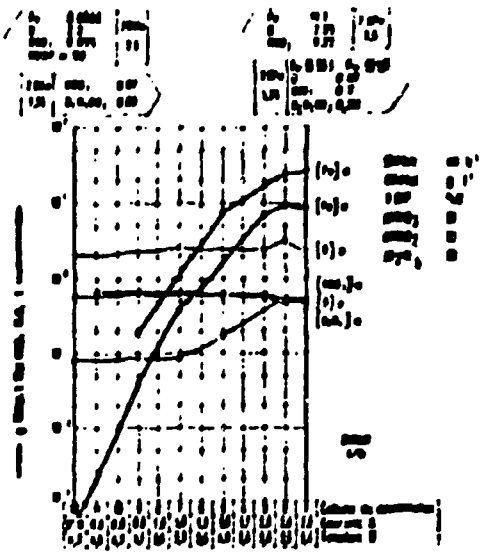

Figure 18: Battery 28-EMMA, profile [illegible] hours, T = 41(2BP), 38(2BW) °C

Figure 18 shows the concentration profiles and gives the partial currents used for the 12 chambers. During the tests performed with the mixer-settler, the ion NH^{+}_{4} was sought in the plutonium solution produced, 2BP, which gives an indication on the reduction efficiency of Pu(IV) by hydrazine according to equation [20]. These analyses revealed concentrations of ammonium ions reaching 0.35 M. This confirms the mechanism described by equation [21].

CHAPTER IV

DISCUSSION OF RESULTS

IV - 1. Comparison of results with the classical processes

As to the quality of the raffinate (concentration of plutonium remaining in 1BU and 2BW) and the concentration of plutonium produced, fixed compared to the flow ratio achievable 1BF/1BXS and 2BF/2BS (2BX), the results presented in tables 6 to 8 surpass by far this which, to our knowledge, have been obtained in industrial facilities (54).

In the EUROCHEMIC facility[5], The U/Pu separation is done in a pulsed column, supplied with U(IV), a reducing agent produced externally and having approximately 8 theoretical stages in the BX portion.[6] As a general rule, very large excesses of U(IV) must be used (10-20 times the stoichiometry) and, despite the number of stages available, only very mediocre decontamination factors of 100 - 500 are obtained.

On the other hand, our electroreduction mixer-settler, equipped with only 6 theoretical stages, has reached decontamination factors of 400-1500. No matter what technique is used (columns or mixer-settler), it is known (private communication) that the reduction efficiency by external U(IV) can be considerably

---

[5] Reprocessing facility at Mol in Belgium

[6] In the case of the reextraction of U(VI), this value of the theoretical number of stages is what corresponds to the McCABE-THIELE simplified model. In our own experiments performed in 1982 with a pulsed column without disphragm (54), we obtained decontamination factors of 10^4 to 10^6. In that case, there were approximately 10 theoretical stages (55).

improved by optimizing the chemical and technical processes. For fuels with a high Pu content (breeder), however, there remains the great disadvantage mentioned above of having to continually recycle over 50% of the total fuel in the form of U(IV).

The results of the elimination of the uranium from the plutonium in the BS portion of the mixer-settler, for the number of stages used, are in good agreement with the predictions based on the distribution equilibria (see IV-3), as well as with those obtained in the classical industrial facilities.

The comparison of the results of the EUROCHEMIC process and of the WAK process using dilute HNO_3 for the reextraction of the plutonium (second Pu cycle), with those of our electroreduction mixer-settler show a still more pronounced improvement. With the first, during the reextraction with diluted HNO_3, decontamination factors of a maximum of 300 are recorded, but they are most often much lower, for approximately 10 theoretical stages. As a general rule, the plutonium concentration produced does not reach over 15 g . l^{-1}. Tables 7 and 8 indicate, on the other hand, that with electroreduction mixer-settlers, the decontamination factors are 10^4 or more for a produced plutonium concentration of 40 $g.l^{-1}$.

IV - 2. Qualitative Description of Simultaneous Processes in the Electroreduction Mixer-Settler

The exchange of matter in the electroreduction mixer-settler is regulated by two simultaneous principal processes:

-- Transfer during extraction

-- Reduction

IV - 2.1. Extraction

Extraction is determined by complexing equilibria of the various components by the TBP and nitric acid in the aqueous phase (see IV - 3.1.1.). Simply speaking, the partition coefficient $_aD$ gives an indication on the distribution of the components for low concentrations of metal ions. This coefficient decreases for the components involved in the process in the following order:

$$U(IV) > Pu(IV) \quad HNO_2 > (U(IV) > HNO_3 >> Pu(III)$$

For U(VI) D is maximum at the concentration of 5 M in HNO_3. Around 0.5 M HNO_3. The values of D drop below 1 for all the components, a fact that will be used for the reextraction of U and Pu. The high value of the partition coefficient of HNO_2 (10) plays an important role in understanding the reoxidation operation. In fact, as we have seen, a portion of the HNO_2 produced in the aqueous phase is transferred in the organic phase where it oxidizes Pu(III) and U(IV). In addition, in the distribution equilibria, it must be considered that $N_2H_5NO_3$, as well as NH_4NO_3 formed by the reduction of Pu(III) by $N_2H_5NO_3$, displaces the aqueous complexing equilibrium towards non-dissociated extractable species ($Pu(NO_3)_4$, $UO_2(NO_3)_2$) and in this way raise the partition coefficients of the metals (salting out effect). A similar effect is observed for Pu(III) which, at greater concentrations, provokes a very large increase of the partition coefficients of the extractable metals (12).

The rate of mass transfer between the aqueous phase and the organic phase has been studied by BAUMGAERTNER (18) by the method of the single drop for Pu(IV),

U(VI), HNO_3. It is quick by comparison to the majority of the redox reactions discussed and can be described by the following relationship:

$$\frac{dC_{org}}{dt} = u_{org} \cdot \rho \left[D C_{aq} - C_{org} \right] \qquad [41]$$

force motrice

with:

$$C_{org} (t = \infty) = D\, C_{aq} (t = \infty) \qquad [41a]$$

$$u_{org} = \frac{Q_{org}}{V_{org}} = \frac{6}{d_T} \qquad [41b]$$

In the case of an infinitely small ($D \rightarrow 0$) partition coefficient, equation [41] is simplified as follows:

$$\frac{dC_{org}}{dt} = -u_{org}\, \beta\, C_{org} \qquad [41c]$$

By integration, the following is derived:

$$\ln \frac{C_{org\,1}}{C_{org\,2}} = u_{org}\, \rho\, \Delta t \qquad [41d]$$

With Ω_{org} = specific transfer surface (cm^{-1})

β = transport constant ($cm \cdot min^{-1}$)

D = partition coefficient

O_{org} = surface of the organic phase (cm^2)

V_{org} = Volume of the organic phase in a mixing chamber

d_T = drop diameter (cm)

Besides time, equation 41d contains the transfer surface determined by the size of the drop and the ratio of the volumes of the two phases in the mixing chamber. If this surface is not sufficiently large and for usual times, efficiency by stage drops below 100%. That is the reason for the very mediocre efficiency of the laboratory mixer-settler (MILLI-EMMA). In fact, in a plexiglas model of the latter we observed drop dimensions up to several millimeters in diameter. The proportion of the phases in the mixing chamber is also unfavorable so that only a very small transfer surface is available. For this surface, times [7] of 1.1 and 2 minutes respectively (see table 5) are insufficient to reach equilibrium. The hypothesis is clearly confirmed by test 33 (table 6), where the time was doubled, which reduces the remaining plutonium concentration in BU and, therefore, promotes obtaining a high decontamination factor.

For a drop diameter d_T = 0.3 cm and β = 0.09 $cm \cdot min^{-1}$ (typical value for the single drop method (18) for example, it is calculated that the half-transfer time rises to 0.7 min. This time is not negligible compared to the normal time of 1 to 2 minutes for the organic phase. Therefore, an incomplete establishment of equilibrium must be expected.

[7] The average times have been calculated assuming that the folumetric ratio of the phases is equal to the corresponding flow ratio. If this hypothesis is not correct, the time of a phase can be a lot shorter.

For the plutonium reextraction experiments (table 7), in the laboratory apparatus the materials transfer conditions are more favorable because the total flow (2BF + 2BS) is automatically reduced, and because the flow ratio 2BF/2BS is a maximum of 3.5, a value for which it is noted experimentally that the transfer surface that is established is larger (better dispersion) than for a larger flow ratio (varying from 7.1 to 9.3 for the U/Pu separation, Table 6).

In the industrial electroreduction mixer-settler (WAK-EMMA), there exist conditions that are more favorable to matter transfer since the efficiency by stage is much better because of the use of a pump mixer and an internal recycling of the aqueous phase in the settling chamber. In addition, at least for the tests in table 8, reduced flow rates have made it possible to reach longer times than in the laboratory mixer-settler. Comparison of the plutonium concentrations on the 2BW raffinates indicates that the concentration in 2BW of the WAK-EMMA is generally lower and, therefore, that the decontamination factor is higher, probably for this reason. For this comparison, however, the results of tests 22 and 27 in table 7 must be put aside for two reasons. Firstly, these tests were performed with a high dibutyl phosphate concentration for which there exists a stable organic complex of Pu(IV) that can, therefore, be reextracted quickly enough by action of the U(IV) formed electrochemically (53). Secondly, they correspond to a very small concentration of uranium in 2BF (< 0.13 g . l^{-1}) which must also lead to a high plutonium concentration in the raffinate.

IV - 2.2. Reduction

The degree of advancement of the reduction is the electroreduction mixer-settler is determined by four processes:

1) direct electroreduction of Pu(IV) according to equation [27]
2) Electroreduction of U(VI) to U(IV) and the reduction of Pu(IV) by U(IV) in the organic and aqueous phases, equations [28], [6], [8].
3) Catalytic reduction, induced electrochemically, of Pu(IV) by hydrazine, equation [30].
4) Autocatalytic reoxidation of Pu(III) and U(IV) extracted in the organic phase, equation 39.

The contribution of each reduction reaction to the overall efficiency must depend on exterior parameters such as the flow, time, the U/Pu proportion, the nitric acid concentration in BF and 1BXS or 2BS, the hydrazine concentration in 1BXS or 2BS, the current intensity imposed and the temperature, as well as on internal parameters such as the effective cathode surface, the current density and the local concentrations of Pu, U, HNO_3 and $N2_{H5+}$. A quantitative description of the complex phenomena in the counter-current extractor by simulation of electronic calculator will be attempted in the following section. A semi-quantitative image of partial outputs can, however, be given using the pseudo-first order approximation, which is valid if the reducing agent is in great excess.

Table 9 gives the pseudo-first order constants estimated by this method as well as the semi-reaction times of the direct electroreduction of Pu(IV), of the reduction of Pu(IV) by U(IV) formed electrochemically and of the catalytic reduction (electrochemically induced) of Pu(IV) by hydrazine.

As for the electroreduction of Pu(IV), we have adopted as β, the transport constant, the value of 0.1 cm . min^{-1} located between the values obtained with a slow agitation and at rest (see Table 3). The difference of the [illeg.] of semi-reduction of Pu(IV) between the WAK-EMMA and MILLI-EMMA apparatus is the result of the difference of specific cathode surface (see table 5). For the electroreduction of U(VI) to U(IV), we made a pessimistic selection of the value of β = 0.005 cm . min^{-1}, among those given in (26).

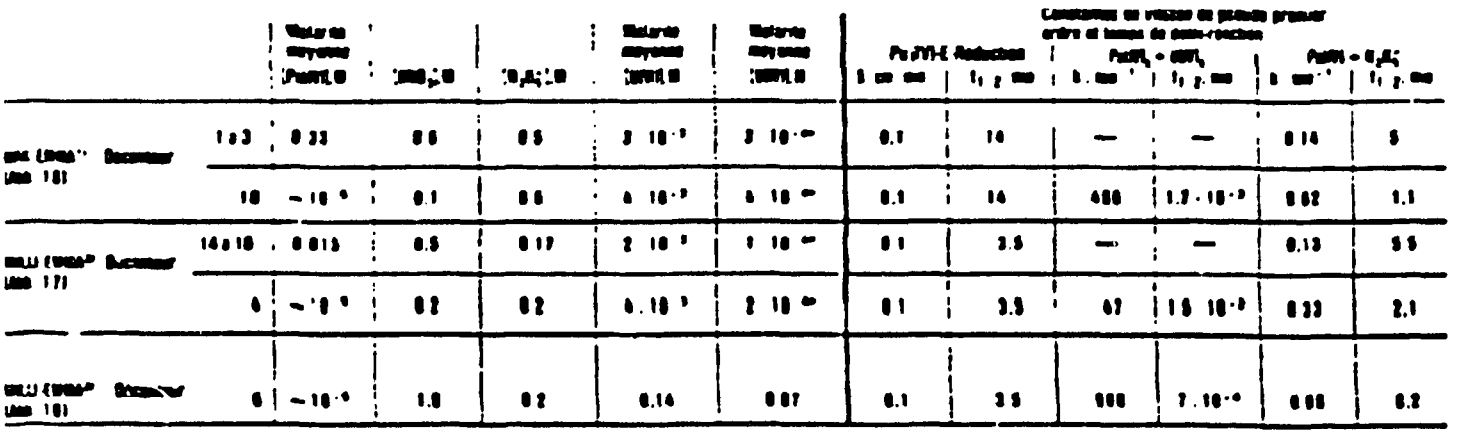

Figure 9: Evaluation of the semi-reaction times in the mixer-settler for direct electroreduction of Pu(IV), the reduction of Pu(IV) by U(IV) and the catalytic reduction of Pu(IV) by hydrazine.

The average concentrations of U(VI) and Pu(IV) in the settling compartments have been estimated from concentration profiles (figures 16-18) using the mass balance equation (equation A /) . It appears that, on the plutonium-rich side, since the approximation consisting of considering the reduction of Pu(IV) by U(IV) as a pseudo first order is not valid, since U(IV) is not in excess in this area of the mixer-settler. [sic] On the contrary, in the plutonium-poor area, this approximation is valid because of the quantity of U(IV) which is ten times in excess. The constant of pseudo first order k of the reduction of Pu(IV) by U(IV) is 3711 M l^{-1} at 20° C. It has been estimated at 30° C and 35° C using an activation energy of 104 kJ . mol-1. The semi-reaction time of reduction of Pu(IV) by hydrazine has been calculated using equations 30 and 31 and the constants from table 4. They are shown on table 9. The following conclusions can be drawn from them:

-- For temperatures above 25°C, in the absence of uranium and for sufficiently large specific cathode surfaces, we can count on an efficiency of Pu(IV) reduction almost as great for direct electroreduction as for reduction by catalysed hydrazine, as we saw in the electroreduction apparatus.

-- For smaller specific cathode surfaces (< 2 cm-1), the part taken by the reduction by hydrazine is dominant (WAK-EMMA).

-- In the presence of small quantities of uranium in the plutonium (U/Pu < 1), as is the case during the reextraction of the plutonium, the reduction in the plutonium poor part of the mixer-settler is done by the U(IV) formed electrochemically, as the semi-reaction times of 10-3 to 10-2 attest.

-- In the presence of large quantities of uranium in the plutonium as during the U-Pu separation, the reduction reaction is almost exclusively due to U(IV).

-- The catalytic reoxidation of Pu(III) and U(IV) (equation 38) will only reach a measurable degree of advancement in the separated organic phase. In fact, because of the rapidity of material exchange (equation 41) and because of the reaction of HNO2 with N2H5+ (equation 15) in the aqueous phase, only low concentrations of HNO2 are present in the organic phase of the mixing chambers.

IV - 3. Quantitative Description of Phenomena by Simulation

The the next few paragraphs, we are attempting to describe the phenomena that are taking place in our mixer-settler using a model that accounts for the extractive transfer and all of the oxidation-reduction reactions. Starting with measurements of the distribution equilibrium between phases and kinetics experiments of oxidation-reduction transfer described above (chapter II and III), the operation of the mixer-settler has been simulated on a computer by the simultaneous solution of all the final equations (19, 57). The original model that we published in 1981 (56) was improved afterwards, principally in the area of the oxidation kinetics (equation 39). This model is based on four basic hypotheses:

1) Extractive transfer (material exchange) takes place only in the mixing chambers and not in the settling chambers (small exchange surface).

2) The chemical redox reactions take place in the mixing chambers as well as in the settling chambers in the two phases.

3) The electroreduction of Pu(IV) and U(VI) takes place in the aqueous medium only in the settling chambers.

4) Finally, it is assumed that the mixing is perfect within each phase (no concentration gradient).

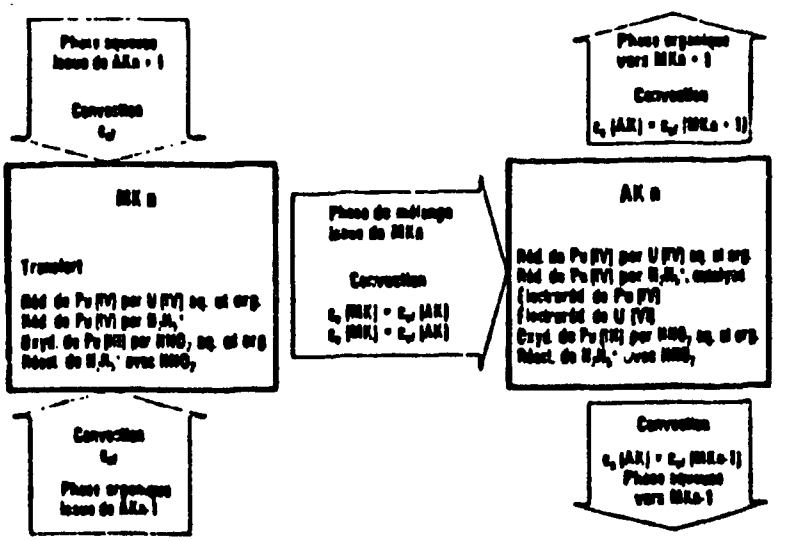

Table 10 Operating model of a mixer-settler stage. MK - Mixing chamber, AK - settling chamber.

A schematic drawing of the model is shown in Table 10 for a stage n of the mixer-settler in communication with the stages n - 1 and n + 1. For a mixer-settler (groups of discrete co-current stages), the counter-current extraction can be assimilated to a counter-current cascade composed of co-current

elements. It is described by a system of algebraic equations for the distribution equilibrium and by differential equations for the transfer kinetics and the redox reactions (19). The mixing and settling chambers are in communication via the transfer term. The oxidation-reduction reaction rates are added separately for each phase to the rates of transfer and convection.

Tables 11a through 11c show the structure of the model. The rate equations used for convection, extractive transfer between phases and the redox reactions are enumerated with indications of their location for the aqueous and organic phases separately.

In Tables 11a and 11b, the concentrations C_A are related to each individual component of the reaction being considered. The constants k_{la} and k_{lo} that are there will, therefore, have different values, depending on the stoichiometry of the reaction depending on the components considered (U(IV), Pu(IV), U(VI), Pu(III), HNO_3, HNO_2, $N_2H^+_5$).

These values are given at 35°C in Tables 11c and 11d. The influence of HNO_3 has always been neglected (k = 0). As for the organic phase, according to (31) for the reduction of Pu(IV) by U(IV) a rate constant equal to 1/100 of its value in the aqueous phase was assumed (see I - 2.2.).

The complete equation system is solved by classical numerical methods (57). For an electroreduction mixer-settler with 16 stages, this system includes over 500 algebraic and differential equations.

Table 11a: Rate equations for the aqueous phase,

AK = settling chamber, MK = mixing chamber

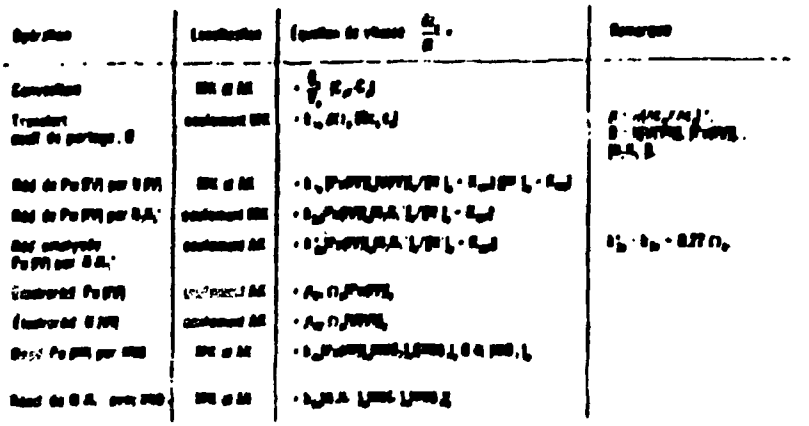

Table 11b: Rate equations for the organic phase

AK = Settling chamber, MK = mixing chamber

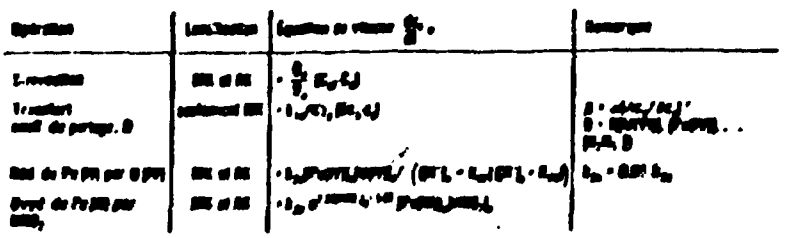

Table IIc: Rate constants k and β for the aqueous phase

Dimensions in cm - Mol- Min; T = 35°C

Constants \ Concentration ϕ_i							
k_{1a}	-1	-1	-1	-1	-1	-1	0
k_{2a}	14000	-20000	0	-14000	20000	0	0
k_{3a}	0	0.073	0	0	0.073	0	-0.073
k'_{3a}	0	$(0.073-0.73\pi_a)$	0	0	$0.073-0.73\pi_a$	0	$(0.073-0.73\pi_a)$
k_{4a}	0	0.1	0	0	0.1	0	0
k_{5a}	-0.033	0	0	0.033	1	0	0
k_{6a}	0	200	0	0	-200	104	0
k_{7a}	0	0	0	0	0	40000	-40000

Table IId: Rate constants k and β for the organic phase

Dimensions in cm-Mol-Min; T = 35°C

Constants \ Concentration ϕ_i							
k_{1o}	1	1	1	1	1	1	0
k_{2o}	150	200	0	-150	200	0	0
k_{3o}	0	1	0	0	-1	0.5	0

Table IIe: Definition of symbols in the tables

- ϕ - Order
- V - Volume of phase
- C - Concentration of an organic species
- β - Coefficient of transport for ion species
- β_0 - Coefficient of transport for electroneutrality
- β - Coefficient de partage $\beta = \frac{C_o}{C_a}$ I
- Ω - Surface de transport/volume de phase (sort optiquement)
- Ω_0 - Surface extractique/volume d'hydrolyte (sort optiquement)
- k_{ia}, k_{io} - Constantes d'hydrolyse pour Hg et U

Indice a : Phase aqueuse
o : Phase organique
I : Interface d'extraction entre la chambre de mélange et de décantation

IV - 3.1. Comments on the structure of the model

IV - 3.1.1. Distribution equilibrium

The distribution equilibrium between phases is determined by all of the components, including by those that are not complexed by the TBP, because of the influence of complexation in the aqueous phase (salting out). The final expressions of the partition coefficients are therefore a function of all of the concentrations. From a large number of distribution measurements and using algebraic equations expressing the partition coefficients of each component, PETRICH et al. (15) have established empirical equations giving the "complexing constants" as a function of all the concentrations. Thus, the distribution equilibrium can be described with good precision (15).

In order to illustrate the formalism used, we will develop here the establishment of the equation of the partition coefficient of U(VI) in the binary system $UO_2(NO_3)_2$ - HNO_3 - TBP. The two components form complexes with TBP according to the following equations:

$$UO_{2a}^{++} + 2NO_{3a}^{-} + 2TBP_o \rightleftharpoons [UO_2(NO_3)_2 \cdot 2TBP]_o \qquad [42]$$

$$H_a^{+} + NO_{3a}^{-} + TBP_o \rightleftharpoons [HNO_3 \cdot TBP]_o \qquad [43]$$

The complexing constants are written as follows:

$$k_U = \frac{|UO_2(NO_3)_2 \cdot 2TBP|}{|UO_2^{2+}|\,|NO_3^-|^2\,|TBP|^2} \; ; \; k_H = \frac{|HNO_3 \cdot TBP|}{|H^+|\cdot|NO_3^-|\,|TBP|} \qquad [44], [45]$$

The partition coefficients are defined by:

$$D_U = \frac{|UO_2(NO_3)_2 \cdot 2TBP|}{|UO_2^{2+}|} \; ; \; D_H = \frac{|HNO_3 \cdot TBP|}{|H^+|} \qquad [46], [47]$$

Whence, the following result:

$$D_U = k_U\,|NO_3^-|^2\,|TBP|^2 \; ; \; D_H = K_H\,|NO_3^-|\,|TBP| \qquad [48], [49]$$

The TBP concentration in equations 48 and 49 is the free TBP concentration, which can be calculated from the total concentration $|TBP|_q$:

$$|TBP| = |TBP|_q - |HNO_3 \cdot TBP| - 2\,|UO_2(NO_3)_2 \cdot 2TBP| \qquad [50]$$

After introduction into equation 48 and transformation, the following is obtained:

$$D_U = \frac{|TBP|_q + A}{2\,|UO_2^{2+}|}\left[1 - \sqrt{1 - \frac{|TBP|_q^2}{(|TBP|_q + A)^2}}\right] \qquad [51]$$

$$A = \frac{(1 + K_H\,|H^+|\,|NO_3^-|)^2}{4K_U\,|UO_2^{2+}|\,|NO_3^-|^2} \qquad [52]$$

As long as the uranium concentration remains low ($\sim 10^{-2}$ M), the complexing constants are almost constant and are as follows:

$K_U = 4.93$; $K_H = 0.04$

IV - 3.1.2. Transfer Rate and By-Pass Model

The equation giving the transfer rate was discussed in section IV - 2. It is a simplified relationship in which the transport coefficients β are variable. PETRICH (19) has shown that they obey the empirical relationship:

$$\beta = \alpha \left(\delta C_o / \delta C_a \right)^{-\gamma} \qquad [53]$$

(α = 0.23± 0.054 cm . min^{-1}, γ = 0.63± 0.16; $\delta C_o / \delta C_a$ = slope of the equilibrium curve in the case where the organic phase is the dispersed phase).

This equation takes good account of the measurements on a single drop for Pu, U, HNO_3, at various TBP concentrations.

Instead of using the coefficient β the incomplete establishment of equilibrium in the mixing chamber can be more simply described from a a bypass model. In this model, it is assumed that a given percentage of fluid traverses the mixing chamber without exchange. This model was used in our simulation tests (see IV - 3.2.).

IV - 3.1.3. Oxidation-reduction Reactions

In the mixing chambers for the reduction of Pu(IV) by hydrazine, the non-catalysed reaction was selected since no platinum deposit is to be suspected here. Given the construction of the anode cell, it is certain the the reoxidation of Pu(III) at the anode can be neglected. That is why no corresponding term has been introduced into the mode. That is also valid for anode oxidation

of hydrazine. On the other hand, hydrazine deterioration by its reaction with the nitrous acid (equation [15]) is taken into consideration (33).

As for the oxidation of Pu(III) by HNO_2, equation 18 has been modified by replacing the concentration of $|HNO_3|$ by the factor $|HNO_3| - 0.4$ to account for the observation in which the oxidation rate is nil for an acid concentration less than 0.4 M.

For the formation of U(IV) by electroreduction (equation [28]), an average transport coefficient β_K of 0.008 cm . min^{-1} (26) was assumed. Likewise for the electroreduction of Pu(IV), the value of 0.1 cm . min^{-1}, the average of those for the electrolyte at rest and agitated, was adopted.

IV - 3.2. Results of the Simulation

IV - 3.2.1. Comparison with Experience

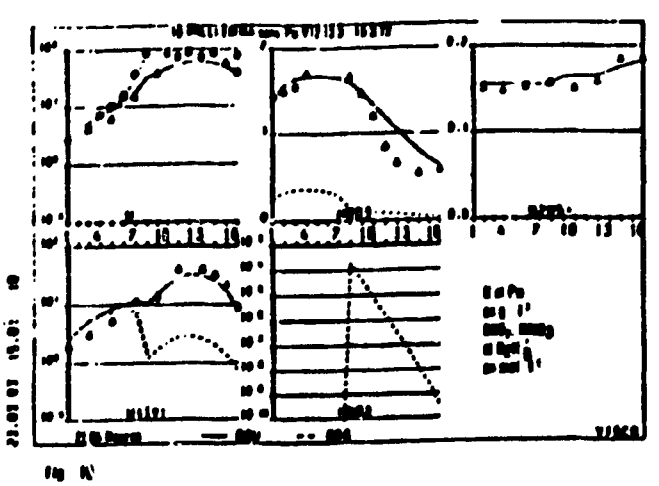

Figures 19 and 20: Comparison of the calculated values (curves drawn) with the measured values (circles, triangles) in the case of a 10 stage mixer-decanter.

Figure 19 shows the results of one of the first tests of the MILLI-EMMA electroreduction mixer-settler. The curves give the distribution of the concentrations of the various components in the facility stages. For uranium, the concentrations are given in g . l^{-1} for HNO_3 and $N_2H_5^+$ in mol . l^{-1}. The circles symbolize the concentrations measured in the organic phase and the triangles, those measured in the aqueous phase. In this experiment the extraction efficiency of the mixer-settler was tested with uranium, in the absence of plutonium. Nine compartments operated in the BX regime and the other seven in BS regime. The organic feed solution 1BF (875 cm^3 . h^{-1} containing $|U(IV)|$ = 86.2 g . l^{-1}, $|HNO_3|$ = 0.12 M and $|HNO_2|_o$ = 0.001 M) was introduced into compartment 9 and the washing solution 1BXS (90 cm^3 . h^{-1} at 30% Vol TBP, $|HNO_3|_o$ = 0.047 M) into chamber 1.[8] Only chambers 12 and 16 were supplied with current. The current densities exceeded 5 $mA.cm^{-2}$.

In addition to the data in Table 5, the following hypotheses were made for the simulation:

— Volume of the aqueous phase per mixing chamber: 6.7 cm^3

— Volume of the aqueous phase per settling chamber: 10 cm^3.

— [illeg]

— Efficiency per stage 80% (bypass model).

The dotted and solid line curves of the same figure 19 show the results of the simulation for the organic and aqueous phases. The excellent agreement for the total concentration of uranium in organic medium is particularly remarkable.

[8] Aqueous mother solution, 1BXS was introduced into compartment 16 (90 cm^3 . h^{-1}, /HNO_3/ = 0.6 M, / N_2H^+[?]/ = 0.18 M).

An equally good agreement is recorded for the hydrazine concentration, while the calculated concentrations |U(IV)|a and |U|a exhibit larger differences from the measurements. However, they still describe the process faithfully. The significant differences of |HNO_3| concentrations in the BX part are perhaps the result of experimental errors rather than an insufficiency of the model.

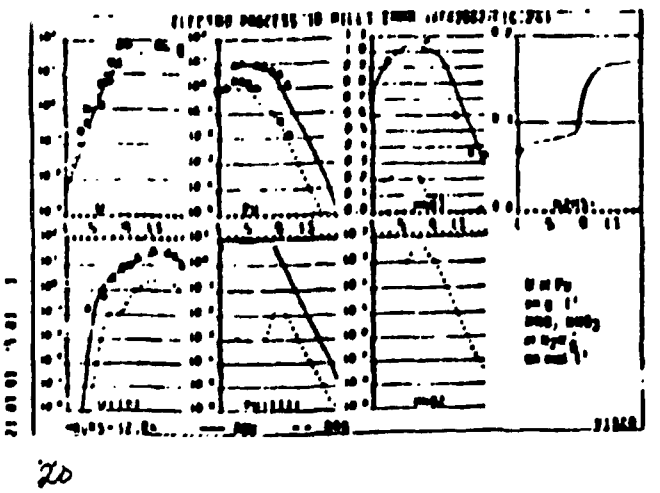

In Figure 20 with the same coordinates as in the preceding figure 19, the measurements of a test with plutonium (No. 14, see figure 15) are compared to the results of the simulation for which the following additional hypotheses were made:

— Volume of the aqueous phase of the mixing chamber: 1 cm^3

— Volume of the aqueous phase in the settling chamber: 6 cm^3

— T = 30°C (corrected constants)

— Efficiency per stage : 80% (bypass model)

— HNO_2 1BFo + 1BSX - 0.005 M

The volumes of the aqueous phase were estimated visually. The concentration in the organic phase adopted for $|HNO_2|_o$ is a mean high value of several experimental measurements.

The simulation shows good agreement between the measured and simulated values - for the Pu concentrations in the organic and aqueous media. It confirms the power of the model.

IV - 3.2.2. Application of the model with variation of the parameters

In this section we propose to study the efficiency of separation for various values of the parameters using the model. Given the advantage of the electro-reduction process, specifically for fuels with a high Pu content, it was a breeder fuel containing 11% Pu[9] by mass which was considered in the simulation calculation.

The standard flow chart selected and the mixer-settler characteristics including ten stages are shown on table 12. The form used and the rate constants are identical to those in the previous section.

[9] This typical content is planned for the large breeder reactors of the future if the core and the axial blanket are processed together. Selection of the mixer-settler dimensions corresponds to an annual capacity of approximately 50 T of fuel, which is the equivalent of approximately 2 GW_e per year produced by two large breeders of the SUPER PHENIX type.

Table 12: Flow Chart and Characteristics of the device to study the influences of the parameters:

Breeder Fuel: Mixed oxide with 11% Pu (core + Axial blanket)
Facility capacity: [illeg.] 50 T per year
Electroreduction mixer-settler, 10 stages total 1BX = 6 stages electrochemically active, 1BS = 4 stages
Standard flow chart (see also Fig. 13)

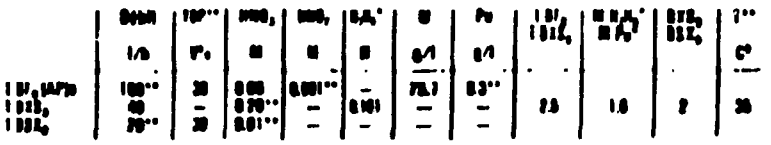

*Constant content by adjustment of [illeg] whatever the variations, if not specified

**Constant whatever the variations

Characteristics of the device	
Total mixer cell volume	4l
Mixer cell volume, aqueous phase	2l
Total settler cell volume	20l
Settler cell volume, aqueous phase	10l
Effective cathode surface	1000 cm^2 (variable)
Efficiency by stage	80% (double flow model)

1V - 3.2.2.1. Influence of the acid concentration in the organic feed solution 1BF$_o$

The simulation results are shown in Figures 21-23 and in Table 13. The acid concentration was varied from 0.06 to 0.2 M.[10]

[10]The range of variation of the acidity corresponds to the effect of mishandling possible in the washing battery of the fission products (HS), which has a decisive influence on the acid concentration of the organic medium (in 1BFo).

Table 13: Influence of parameters

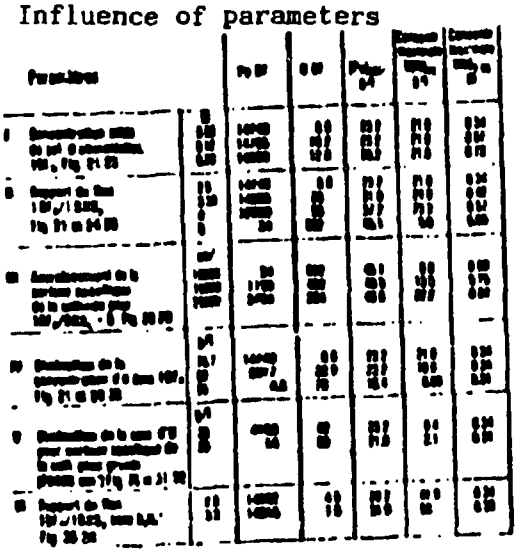

All of the other parameters are those of the standard flow chart. It appears that, for a flux ratio BF_o/BXS_a = 2.5, Pu separation is excellent with a decontamination factor (DF) above 10,000, whereas that of uranium is low, because of the small number of washing stages in the 1BS portion. The effect of the acid concentration on the separation efficiency, at least in the range of variation given, is scarcely perceptible. Thus, the concentration profiles, except obviously that of [illegible], exhibit no difference. These simulation results show amply that the electroreduction mixer-settler can be considered as insensitive to a variation of this parameter.

IV - 3.2.2.2. Influence of an increase of the flux ratio $1BF_o/1BSX_a$

Figures 24-26 and table 13 - II show the results obtained when the ratio BF_o/BXS_a varies from 2.5 to 5.

Figures 21 - 34: Calculated concentration profiles for U, Pu, HNO_3, U(IV), Pu(III), HNO_2 and N_2H_5+ in the case of a 10 stage mixer-settler for various cases:

-- variation of U and HNO_3 concentrations in the organic feed (Figures 21-23 and 29-32)

-- Variation of the flow rato o/a (figure 24-26)

-- Variation of the cathode surface (fig. 27 and 28)

-- Absence of hydrazine (fig. 33 and 34).

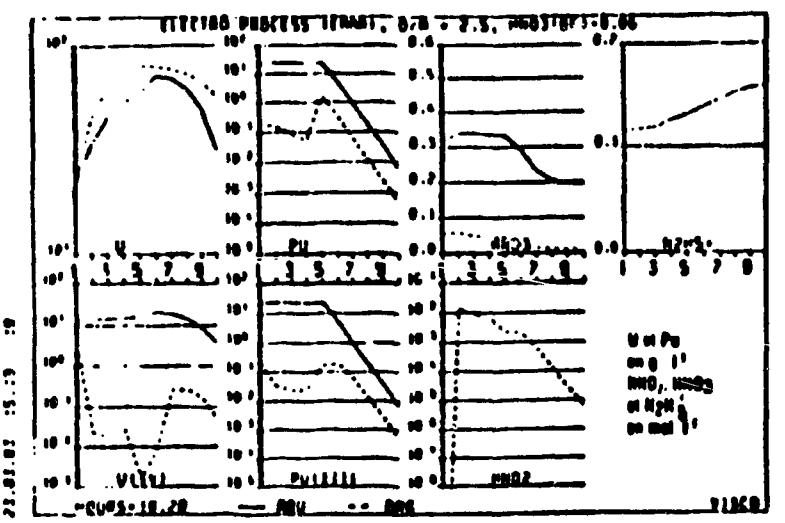

Fig. 24

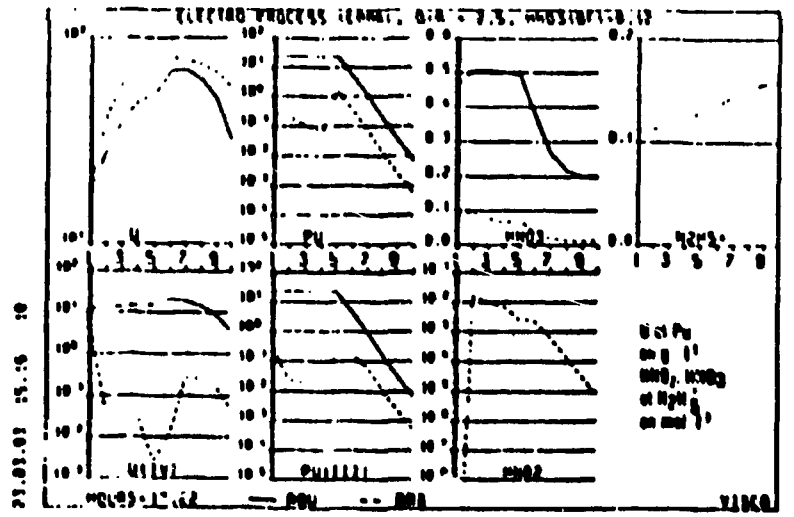

Fig. 22

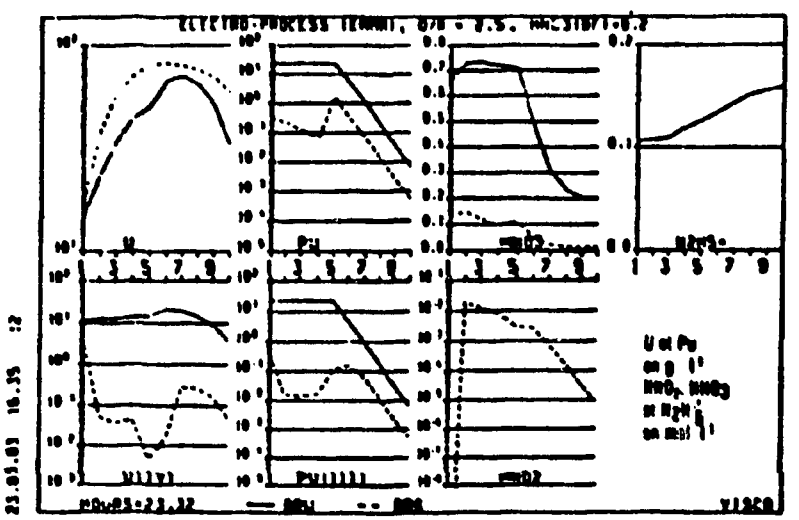

Fig. 23

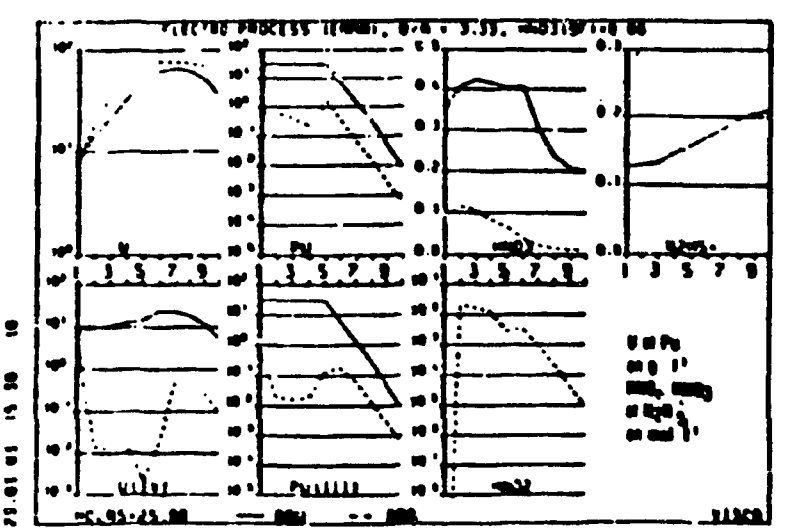

Fig. 24

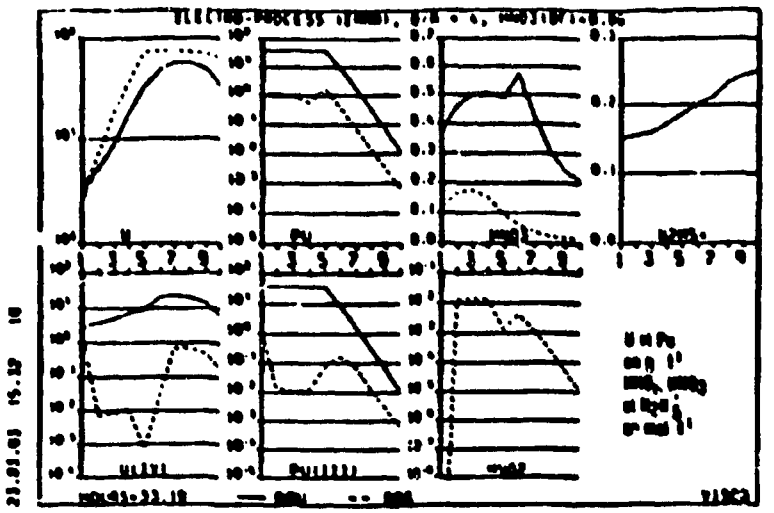

26

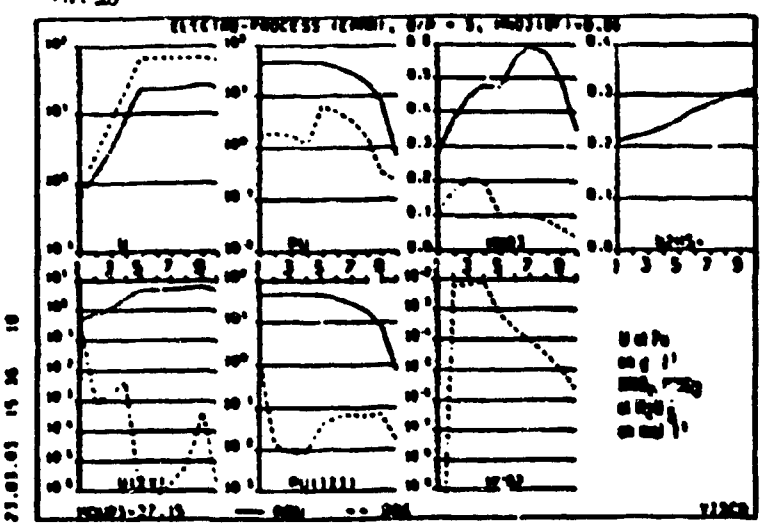

26

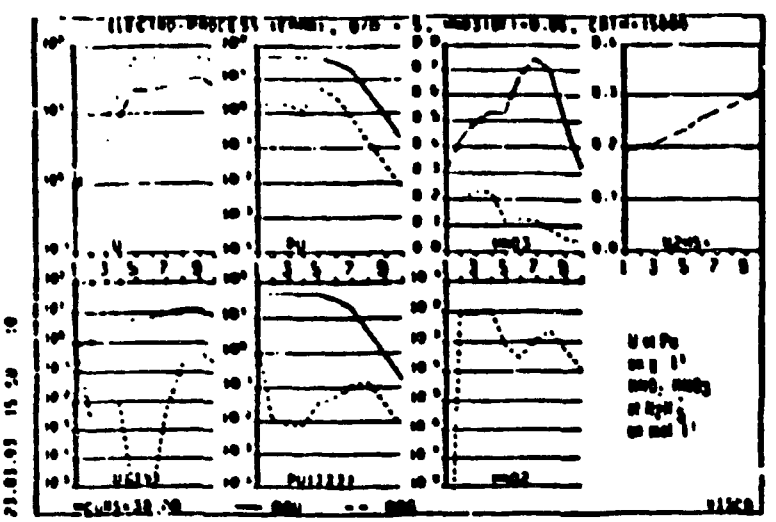

27

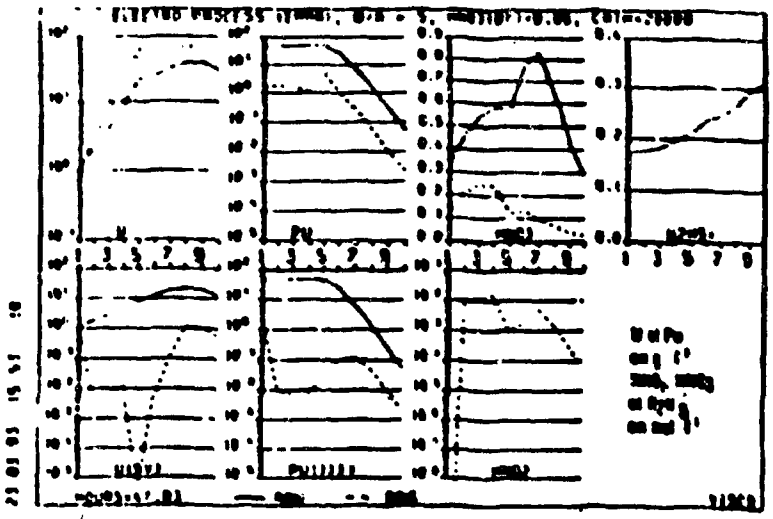

266

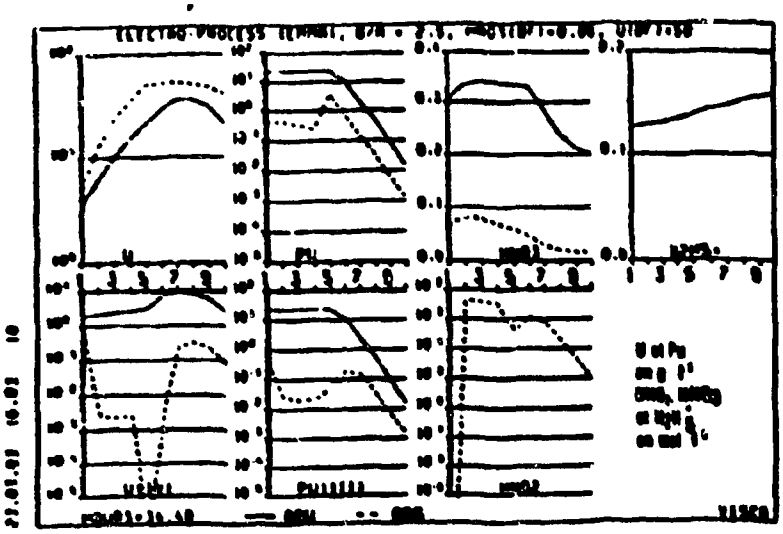

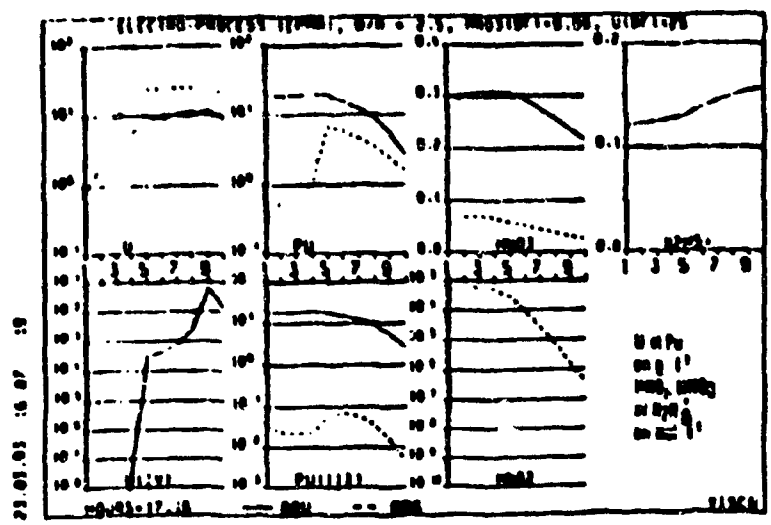

266

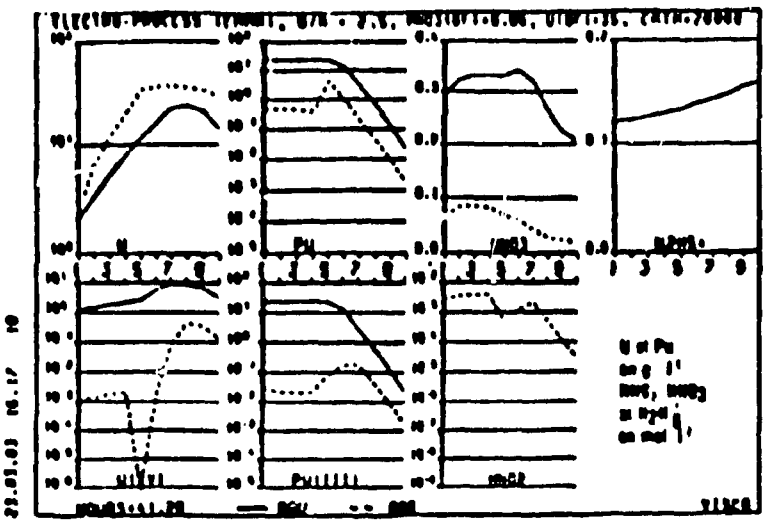

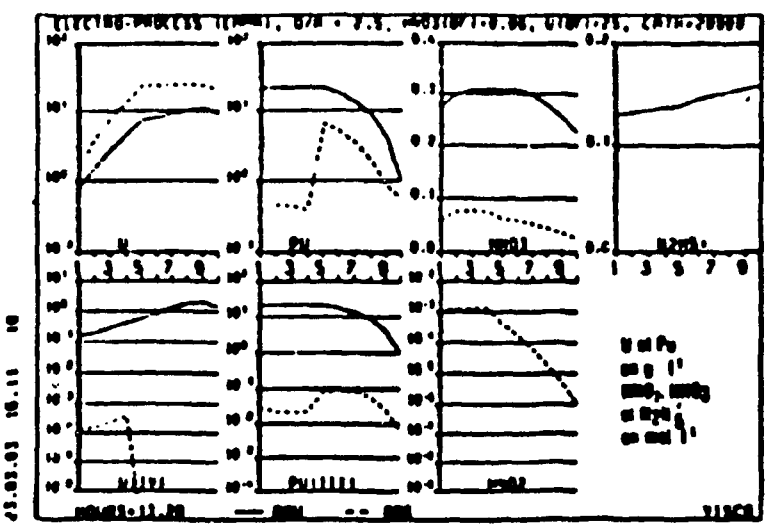

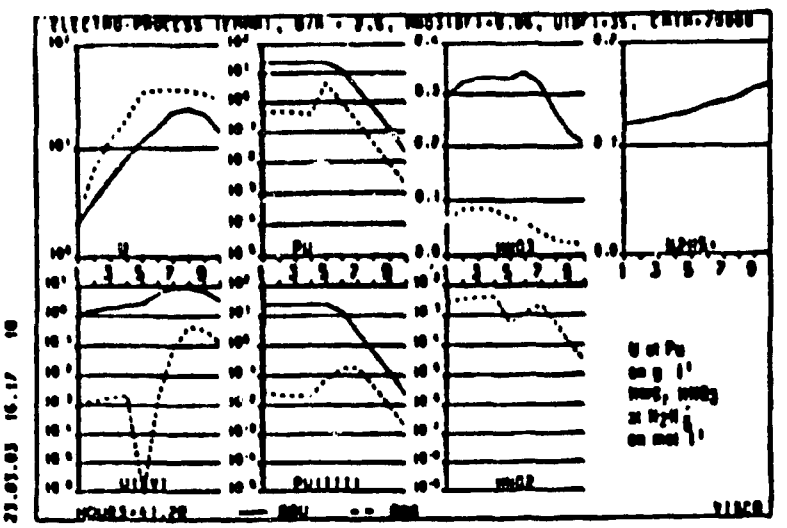

Fig. 31

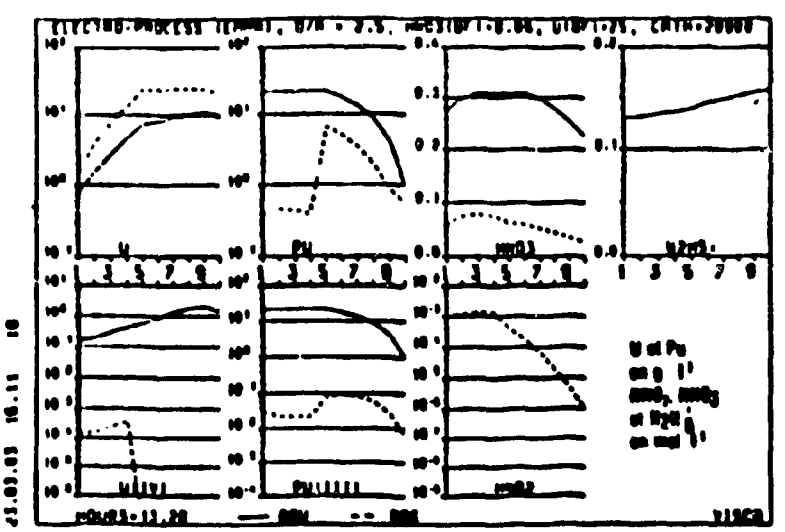

Fig. 32

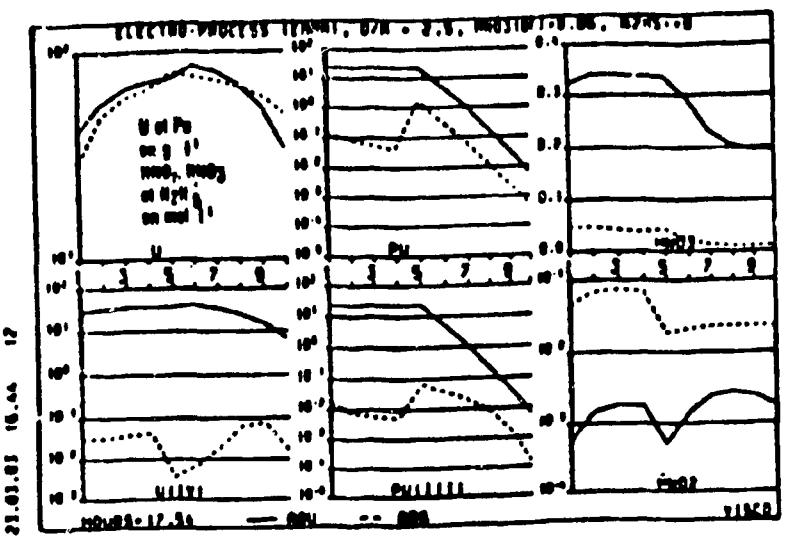

Fig. 33

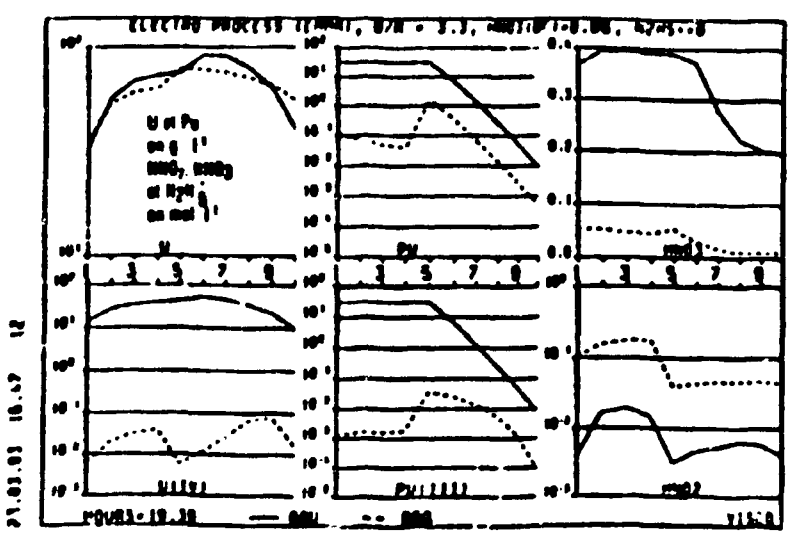

Fig. 34

Up to the value of 4, only a very small effect on Pu separation is observed, whereas the U decontamination factor increases, as was to be expected, because of the increase of the quenching factor. For the flux ratio BF_o/BXS_a = 5, the Pu decontamination factor decreases to an unacceptable value. The explanation of this fact must be sought in the insufficiency of the U(IV) addition. In the entire BX portion, the U(IV) concentration then drops below 10^{-3} g . l^{-1}. Likewise, the aqueous U(IV) concentration in the settling chambers is 10 g l^{-1} from one end to the other (see figure 26). Reoxidation in the organic phase and particularly the insufficient U(VI) addition that can be reduced in an aqueous medium (compare figures 21, 24, 25 with figure 26) caused by the high Pu(III) concentrations in the aqueous medium (salting out) are certainly a cause of the drastic drop of the Pu decontamination factor.

IV - 3.2.2.3. Influence of an increase of the cathode surface

For large facilities, the cathode surface in the mixer-settler can easily be increased by insertion of additional plates of laminated titanium up to a value of Ω_K above 1 (MILLI-EMMA: $\Omega_K \sim 2$). The production of U(IV) is then increased. In figures 26-28 and table 13 III, the influence of the increase of the cathode surface on the decontamination values of plutonium and uranium is studied, for a flux ratio BF_o/BXS_a = 5. As could be expected, the Pu decontamination factor increases. It already exceeds 1000 for Ω_K = 1.5 and for [illeg.] it reaches 3700. Figures 26-28 show clearly the increase in both the total uranium concentration and U(IV) in the aqueous phase. The uranium decontamination factor decreases when the cathode surface increases since the four BS stages are not sufficient for the complete separation of U(IV).

IV - 3.2.2.4. Influence of a decrease of the uranium concentration (U/Pu)

For a fuel with a high plutonium content, it is to be expected that the uranium concentration play an important role in the plutonium decontamination factor, and even more so because only six stages (4.8 theoretical stages for 80% efficiency by stage) are available in the BX portion.

Figures 29 and 30 and Table 13 - IV show the influence of a decrease of the uranium concentration from 50 to 25 g . l^{-1} in $1BF_0$, for a constant plutonium concentration. While the decontamination factor is still 5900 for 50 g . l^{-1}, for 25 g . l^{-1} only 80% of the plutonium is separated. As indicated by figure 30, the number of stages in the BX portion is then insufficient to obtain total separation since reduction is less complete.

Doubling the number of stages should certainly result in a sufficient decontamination factor value, as shown by the plutonium reextraction experiments (see section III - 3.2).

As was to be expected, Pu separation is improved still further by increasing the cathode surface, for small uranium contents, as shown by figures 31, 32, and Table 13 - V.

IV - 3.2.2.5. Electroreduction in the absence of hydrazine

We mentioned that, for 0.4 M concentrations of HNO_3, nitrous acid no longer acts as an oxidizing agent of Pu(III). That is why it should be possible to do electroreduction without adding hydrazine, when the acid concentration in the

extractor is held below 0.4 M. Until now, we have only done preliminary tests of electroreduction without hydrazine in an aqueous medium. The counter-current experiments must still be done. If the modified form of equation 18 (see table 11a) is used in the computer simulation for the oxidation of Pu(III), the model gives the expected result. For a flux ratio BF_o/BXS_a = 2.5 and even 3.3 and for a nitric acid concentration in the organic phase of 0.06 M, a concentration of this acid below 0.4 M in the aqueous phase is established along the entire length of the extractor. Under these conditions, plutonium is effectively separated as shown by figures 33 and 31 and table 13 - VI. With high concentrations of U(IV) in the aqueous phase (50 g . l^{-1} maximum, table 11 - VI), the nitrous acid concentration in the organic medium is 0.2 M, which indicates a conside3rable reoxidation efficiency (figure 33, 34).

CONCLUSIONS

From the experimental tests described in the first part of this research, we were able to construct a compact device capable of performing the double function of extraction and electroreduction for U/Pu separation. A first prototype of this device has been in successful service at the Karlsruhe nuclear fuel reprocessing plant since 1979. In this device, the reduction rate, which depends on the cathode surface and the uranium content, is determined by three concurrent reactions:

1. Direct electroreduction of Pu(IV)

2. The indirect reduction of Pu(IV) by U(IV), U(IV) being itself formed by the direct electroreduction of U(VI).

3. The reduction of Pu(IV) by hydrazine, which is in turn catalysed by the material in the device.

Using our mathematical models, we were able to simulate the degree of advancement of the reaction and the efficiency of the U/Pu separation.

APPENDICES

APPENDIX I

FORM OF THE MULTI-STAGE COUNTER-CURRENT EXTRACTION OF A SINGLE EXTRACTABLE COMPONENT

The partition coefficient is defined by:

$$D = Y/X \qquad [A1]$$

where Y is the concentration of the extractable component in the organic phase and X the concentration in the aqueous phase. The total quantity extracted depends on the volumes used or on the volume flow rates in the aqueous and organic phases. Therefore, the extraction factor is defined as follows:

$$E = \frac{LY}{SX} = \frac{L}{S} \cdot D \qquad [A2]$$

L is the volume or volume flow rate of the light organic phase and S that of the heavier aqueous phase.

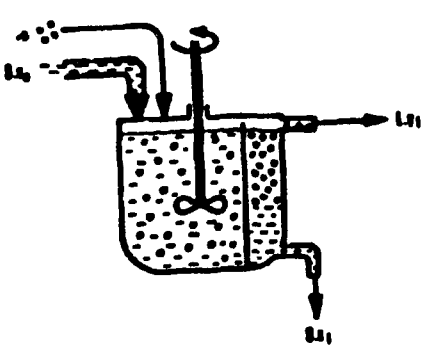

Figure A1-1: One stage extraction of a single component

Figure A1-1 shows the process in a single theoretical stage ("theoretical" means that the partition equilibrium is 100% established). Assuming that the extraction agent used is fresh, that is $Y_o = 0$, and that the extractable component is supplied solely by the mass flow SX_o, the material balance equation is written as follows:

$$SX_o = SX_1 + LY_1 \qquad [A3]$$

from which the fraction extracted is derived:

$$\frac{X_1}{X_o} = \frac{1}{1 + E} \qquad [A4]$$

For a multi-stage extraction, the calculation is more complex.

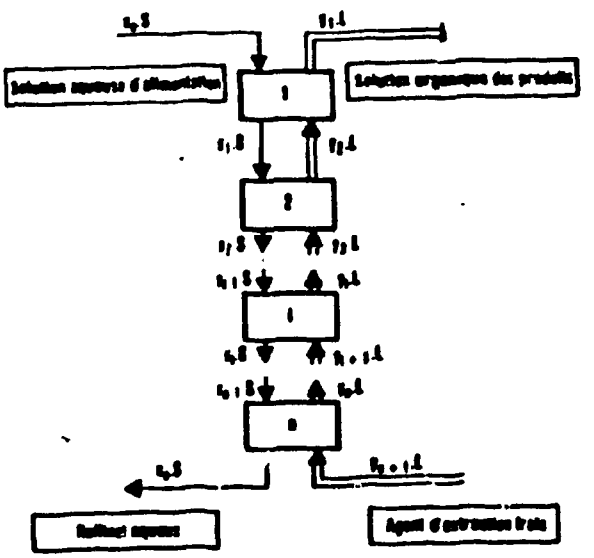

Figure A1-2: Multi-stage counter-current extraction (counter-current extraction composed of [illeg] parallel elements)

Figure A1-2 shows a counter-current cascade composed of n elements. The indices of the exiting concentrations are also the stage numbers. The equation of the material balance for the complete cascade is written as follows:

$$S(X_o - X_n) = L(Y_1 - Y_{n+1}) \qquad [A5]$$

For a fresh extraction agent, or $Y_{n+1} = 0$, we have:

$$Y_1 = S(X_o - W_n) \qquad [A6]$$

The general formula for the material balance in any stage is:

$$S(X_{i-1} - X_i) = L(Y_i - Y_{i+1}) \qquad [A7]$$

Starting from the concentration X_n in stage n, Y_n is calculated first using the partition coefficient $D_n = Y_n/X_n$, then X_{n-1} and so forth for the entire cascade. Finally the number of separation stages required is obtained, that is, the number for which the final aqueous concentration reaches that of the feed organic concentration X_n.

This formalism illustrated the mathematical treatment of a counter-current cascade. For the extraction of several components coupled with oxidation-reduction reactions, the approximation of the stages is no longer valid. An adapted formulation is described in chapter IV.

APPENDIX II

POURBAIX DIAGRAM FOR THE Pu-H_2O and HNO_3-HNO_2-H_2O SYSTEMS (51)

Figure AII-I reproduces the Pourbaix diagram corresponding to the oxidation states of plutonium: Pu(III), Pu(IV), Pu(V), Pu(VI). This figure gives the potential of the pair Pu^{4+}/Pu^{3+} in nitric acid (21), instead of the standard potential as a function of pH. The figure also represents the variation of the pair HNO_3/HNO_2 with the pH. For a pH of 0.2 (point of intersection), the standard potential of the pair NO_3^-/HNO_2 is equal to the real potential of the pair Pu^{4+}/Pu^{3+} and then becomes lower for a higher pH. This fact supports the observation according to which nitrous acid acts as a reducer of Pu(IV) for nitric acid concentrations below 0.4 M.

This diagram also shows the non-existence of Pu(V) in a strongly acid solution, as well as the reducing action of the nitric ion on Pu(VI).

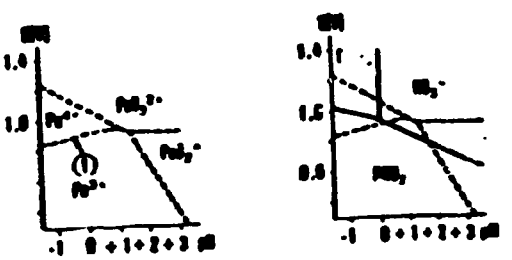

Figure AII-1: Pourbaix Diagrams (51)

APPENDIX III

THERMODYNAMIC EQUILIBRIA CONSTANTS FOR Pu(IV) REDUCTION BY U(IV) AND Fe(II)

The corresponding redox pairs are as follows:

$$Pu^{4+} + e^- \text{ , } E_o = 0.914 \text{ V (real potential in 1 M } HNO_3) \qquad [A8]$$

$$UO_2 2+ + 4H^+ + 2e^- \rightarrow U^{4+} + 2H_2O \text{ , } E_o = 0.33 \text{ V (standard potential)} \qquad [A9]$$

By writing the equality of the potentials, the following equilibrium constant is found for the reduction reaction:

$$K = \frac{|UO_2^{2+}| \; |H^+|^4 \; |Pu^{3+}|^2}{|U^{4+}| \; |Pu^{4+}|^2} = 1.3.10^{20} \quad (20°C) \qquad [A10]$$

For a complete reduction, therefore, only a very slight excess of U(IV) would be required in theory.

The situation is completely different if Fe(II) is used as the reducing agent. The standard potential of the pair Fe^{3+}/Fe^{2+} is 0.77 V. From this value, the equilibrium constant is calculated:

$$K = \frac{|Fe^{3+}| \; |Pu^{3+}|}{|Fe^{2+}| \; |Pu^{4+}|} = 303 \quad (20°C) \qquad [A11]$$

The considerable additions of Fe(II) required in practice for the complete separation of plutonium are therefore justified.

APPENDIX IV

ESTIMATION OF THE ELECTROREDUCTION EFFICIENCY IN THE SETTLING CHAMBER

The integrated formula of equation [27]:

$$t_R = -\frac{V}{F\,\Omega_k} \ln \frac{|Pu(IV)|_{t=0}}{|Pu(IV)|_{t_R}} \qquad [A12]$$

allows the time required to obtain the desired output to be estimated. For example, in order to get 80% of the plutonium by direct electroreduction, with a transport constant of 0.12 cm . min^{-1}, an average between the values for the electrolyte at rest and agitated (see Table 3), and an estimated specific cathode surface Ω of 2 cm^2 . cm^{-3} (Table 5), a required time t_R of 5.8 min is found. This is reached in the laboratory mixer-settler MILLI-EMMA. As indicated by Table 5, it is in fact equipeed with 9 to 12 settling chambers, the real time for the aqueous phase in each chamber is 6 min. the compliment of 100% efficiency of the reduction corresponds to a reduction by U(IV) formed simultaneously. It is, of course, understood, that the average current densities are sufficiently large.

APPENDIX V

ABSORPTION SPECTRA FOR Pu(III), Pu(IV), Pu(VI), U(IV) and U(VI)

The absorption spectra of the individual oxidation states of plutonium and uranium, in the visible and near infrared ranges are shown in figure AV-1. The molar quenching coefficients are shown as ordinates. The relative molar quenching coefficient ΔE was used here. It is defined as the difference between the quenching maximum and a quenching valley (selected at 518 nm for the 380-700 range and at 747 nm for the 700-1200 nm range). This method makes it possible to minimalize the errors brought about by varying the base line.

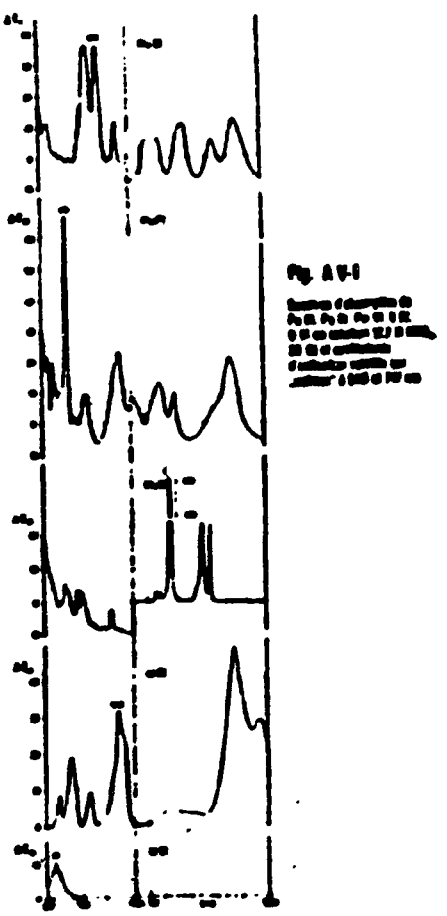

Figure AV-1: Absorption Spectra of [illeg.]

ABBREVIATIONS AND SYMBOLS

PUREX process code:

$1BF_o = 1AP_o$ = Organic mother (or feed) solution

$1BU_o$ = Organic uranium solution produced

$1BSX_o$ = Organic washing solution

$1BSX_a$ = Aqueous mother solution

$1BP_a$ = Aqueous plutonium solution produced

$2BF_o$ = Organic mother solution (second Pu cycle)

$2BW_o$ = Purified organic phase

$2BS_a$ = Aqueous feed solution

$2BP_a$ = Aqueous plutoniium solution produced

D = Partition coefficient

k = Rate constant

K = Hydrolysis constant or equilibrium constant

t = Time

T = Temperature

β = Transport coefficient

i = Current density

i_g = Limiting current density

F = Faraday constant

z = Electrochemical valence

C = Concentration

X = Concentration in aqueous phase

Y = Concentration in organic phase

$|x|$ = Concentration

Q = Flow rate

Ω [?] = Specific surface

l = Length

V = Volume

O_k = Cathode surface

O = Surface

d_T = Drop diameter

$\delta C_{org}/\delta C_{aq}$ = Slope of the equilibrium curve

L = Volume of the organic phase

S = Volume of the aqueous phase

E = Extraction factor

R = Constant of perfect gases

E_o = Standard potential

DF = Decontamination factor

BIBLIOGRAPHY

1 - F. BAUMGARTNER
Kerntechnik, 20 (1978), 74

2 - J. COUTURE, J. MAMELLE, P. AUCHAPT
"Nuclear Power and its Fuel Cycle",
Proceedings Intern. Conf. Salzburg 1977, Vol. 3, p. 579

3 - W.M. LATIMER
"Oxidation Potentials"
Prentice Hall Inc., Englewood Cliffs, N.J. (1959)

4 - R.L. WALSER
US-AEC Report, ARH-SA-69

5 - W. OCHSENFELD, H.J. BLEYL, D. ERTEL
Deutsches Atomforum Dusseldorf, Reaktortagung 1976

6 - F. BAUMGARTNER, E. SCHWIND, P. SCHLOSSER
Deutsche Patentschrift 1905 519 (1970)

7a - H. SCHMIEDER, F. BAUMGARTNER, H. GOLDACKER, H. HAUSBERGER
Deutsches Atomforum, Reaktortagung 1971, Bonn

7b - H. SCHMIEDER, F. BAUMGARTNER, H. GOLDACKER, H. HAUSBERGER
24. IUPAC Congress, Hamburg 2 - 8/9/1973

7c - H. SCHMIEDER, F. BAUMGARTNER, H. GOLDACKER, H. HAUSBERGER, E. WARNECKE
Proceedings Intern. Solvent Extraction Conf., Vol. III, p. 1997, Lyon 1974

7d - F. BAUMGARTNER, H. GOLDACKER, H. SCHMIEDER
in "Actinide Separations", ACS Symposium Series 117, American Chemical Society, Washington 1980

7e - H. SCHMIEDER, H. GOLDACKER, M. HEILGEIST, G. PETRICH
"Fast Reactor Fuel Cycle", British Nuclear Energy Society, Paper n° 47, London 1981

8 - H. HAUSBERGER
Dissertation, Universität Heidelberg (1972)

9 - A. SCHNEIDER, A.L. AYERS
US-Patent 3 616 276 (1971)

10 - Personal Communication

11 - W. OCHSENFELD, G. BAUMGARTEL, H. SCHNIEDER
"Solvent Extraction Research", édité par A.S. Kertes et Marcus, Wiley,N.Y. 1969

12 - H. SCHNIEDER, G. PETRICH, A. HOLLMANN
J. Inorg. Nucl. Chem. 43, 3373 (1981)

13 - W.E. GROENIER
US-AEC Report ORNL-4746 (1972)

14 - H. ROUYER, H. MERLE
Congrès "Emploi des calculateurs électroniques en génie chimique"
Paris, avril 1973

15 - G. PETRICH, Z. KOLARIK
Rapport KfK-3080 (1981)

16 - Z. KOLARIK, G. PETRICH
Ber. d. Bunsenges. f. Phys. Chemie 83, 1110 (1979)

17 - G. PETRICH
in "Modelling of Chemical Reactions"
Springer Series in Chemical Physics 18, Springer Verlag 1981

18 - F. BAUMGARTNER, L. FINSTERWALDER
J. Phys. Chem. 74, 108 (1970)

19 - G. PETRICH
Proc. Intern. Solvent Extr. Conf., Liège, Sept. 6 - 12, 1980
Université de Liège 1980

20 - S.W. RABIDEAU
J. Am. Chem. Soc. 78, 2705 (1956)

21 - P.I. ARTIUKHIN, A.D. GELMAN, V.I. MEDVEDOVSKI
Doklady A.N. SSSR 12, 269 (1958)

22 - E.K. DUKES
J. Am. Chem. Soc. 82, 9 (1960)

23 - D. COHEN
J. Inorg. Nucl. Chem. 18, 207 (1961)

24 - W.E. HARRIS, I.M. KOLTHOFF
J. Am. Chem. Soc. 67, 1484 (1945)

25 - I.M. KOLTHOFF, W.E. HARRIS
J. Am. Chem. Soc. 68, 1175 (1946)

26 - H. SCHMIEDER, F. BAUMGARTNER, H. GOLDACKER, H. HAUSBERGER
Rapport KfK-2082 (1974)

27 - T.W. NEWTON
J. Phys. Chem. 63, 1493 (1959)

28 - S.W. RABIDEAU
J. Am. Chem. Soc. 79, 3675 (1957)

29 - R.M. SMITH, A.E. MARTELL
"Critical Stability Constants", IV
Plenum Press, New York, London (1976)

30 - P. BIDDLE et al.
J. Inorg. Nucl. Chem. 28, 1736 (1966)

31 - P. BIDDLE, H.A.C. Mc KAY, J.H. MILES
Conference "Solvent Extraction of Metals",
Harwell, 27 - 30 sept. 1965

32 - W.J. PLIETH in A.J. Bard
"Encyclopedia of Electrochemistry of the Elements",
Vol. 8, Marcel Dekker Verlag, New York (1978)

33 - P. BIDDLE, J.H. MILES
J. Inorg. Nucl. Chem. 30, 1291 (1968)

34 - W. OCHSENFELD, H. SCHMIEDER
(unpublished)

35 - T. TSUJINO, T. AOCHI
J. Nucl. Science Techn. 13, 321 (1976)

36 - W. OCHSENFELD, H. SCHMIEDER, S. THEISS
Report KfK-911 (1970)

37 - YU-KEUNG SZE et al.
Nucl. Technol. 56, 527 (1982)

38 - V.S. KOLTUNOV, G.I. ZHURAVLEVA
Radiokhimiya 16, 84 (1974)

39 - KfK-IHCH
(unpublished report)

40 - V.P. CARACCIOLO
USAEC-Report DP-896 (1964)

41 - M. HEILGEIST, A. HOLLMANN
Report KfK-HICH, unpublished

42 - D.J. PICKETT
"Electrochemical Reactor Design"
Elsevier Scientific Publishing Comp., Amsterdam 1979

43 - E. BOHNERT (KfK-IHCH)
Personal Communication

44 - C.C. HSIANG, C.T. CHANG
J. Inorg. Nucl. Chem. 37, 1949 (1975)

45 - H. SCHMIEDER, H. GOLDACKER, M. HEILGEIST, M. KLUTH, H. HAUSBERGER, L. FINSTERWALDER
Report KfK-2957 (1980)

46 - M. HEILGEIST
Report KfK-3517 (1983)

47 - KfK-IHCH
Unpublished report

48 - H. SCHMIEDER, E. KUHN, W. OCHSENFELD
KfK- 1306 (1970)

49 - Z. KOLARIK
J. Inorg. Nucl. Chem. 43 (1981)

50 - Personal Communication

51 - M. POURBAIX
"Atlas of Electrochemical Equilibria in Aqueous Solutions"; Pergamon Press, Oxford 1966

52 - D. ERTEL, P. GROLL, G. KNITTEL, W THEISS
J. Radioanal. Chem. 32, 297 (1976)

53 - L. STIEGLITZ, W. OCHSENFELD, H. SCHMIEDER
KfK-691 (1968)

54 - H. SCHMIEDER, H. GOLDACKER, L. FINSTERWALDER
KfK-2615 (1977)

55 - Rapport KfK-IHCH,non publié

56 - G. PETRICH, H. SCHMIEDER
Report KfK-3290 (1982)

57 - G. PETRICH
Proceedings IASTED, Symp. on modelling, identification and control, Davos, 2 -5 mars 1982, p. 49